Available online at www.sciencedirect.com
SCIENCE DIRECT®
Coordination Chemistry Reviews 248 (2004) 321–350
COORDINATION CHEMISTRY REVIEWS
www.elsevier.com/locate/ccr

Review

Photophysical properties of porphyrinoid sensitizers non-covalently bound to host molecules; models for photodynamic therapy

K. Lang [a,*], J. Mosinger [a,b], D.M. Wagnerová [a]

[a] *Institute of Inorganic Chemistry, Academy of Sciences of the Czech Republic, 250 68 Řež, Czech Republic*
[b] *Department of Inorganic Chemistry, Faculty of Science, Charles University in Prague, Hlavova 2030, 128 43 Praha 2, Prague, Czech Republic*

Received 6 October 2003; accepted 10 February 2004

Contents

Abbreviations: AlPcS, sulfonated aluminium phthalocyanine; $AlPcS_n$, sulfonated aluminium phthalocyanine ($n = 1$, 2, 3, 4, number of sulfo groups); BC, bacteriochlorin a; βLG, β-lactoglobulin; BMPyP, 5,10-bis(*N*-methylpyridinium-4-yl)-15,20-bis(phenyl)porphyrin; BPPTP, 5,15-bis(α-triphenylphosphonium-4-tolyl)-10,20-bis(4-tolyl)porphyrin; BSA, bovine serum albumin; CD, cyclodextrin; dAMP, deoxyadenosine 5′-monophosphate; dCMP, deoxycytidine 5′-monophosphate; dGMP, deoxyguanosine 5′-monophosphate; DMPC, dimyristoylphosphatidylcholine; DNA, deoxyribonucleic acid; DOPC, dioleoylphosphatidylcholine; DOPS, dioleoylphosphatidylserine; DPPC, dipalmitoylphosphatidylcholine; DP, deuteroporphyrin; dTMP, deoxythymidine 5′-monophosphate; EPC, egg phosphatidylcholine; HSA, human serum albumin; HP, hematoporphyrin; hpCD, 2-hydroxypropyl-cyclodextrin; HPD, hematoporphyrin derivative; LDL, low-density lipoproteins; $MgPcB_4$, magnesium tetrakis(4-*tert*-butyl)phthalocyanine; MgTBP, magnesium tetrabenzoporphyrin; MPyP, 5-(*N*-methylpyridinium-4-yl)-10,15,20-tris(phenyl)porphyrin; PcS, sulfonated metal-free phthalocyanine; PDT, photodynamic therapy; PdTEPP, palladium (II) 5,10,15,20-tetrakis(pentan-3-yl)porphyrin; PdTMPyP(X), palladium(II) 5,10,15,20-tetrakis(*N*-methylpyridinium-*X*-yl)porphyrin, $X = 2$, 3 and 4; PdTPP, palladium(II) 5,10,15,20-tetraphenylporphyrin; PdTPPS, palladium(II) 5,10,15,20-tetrakis(4-sulfonatophenyl)porphyrin; PO, porphycene; $[poly(dG\text{-}dC)]_2$, double-stranded GC alternating polynucleotide; $[poly(dA\text{-}dT)]_2$, double-stranded AT alternating polynucleotide; POPC, monopalmitoyl-monooleylphosphatidylcholine; PP, protoporphyrin IX; TMPTP, 5,10,15,20-tetrakis(α-trimethylphosphonium-4-tolyl)porphyrin; TMPyP, 5,10,15,20-tetrakis(*N*-methylpyridinium-4-yl)porphyrin; TPPB, 5,10,15,20-tetrakis(3,5-di-*tert*-butylphenyl)porphyrin; TPPC, 5,10,15,20-tetrakis (4-carboxyphenyl)porphyrin; TPPP, 5,10,15,20-tetrakis(4-phosphonatophenyl)porphyrin; TPPS, 5,10,15,20-tetrakis(4-sulfonatophenyl)porphyrin; TPPTP, 5,10,15-tris(α-triphenylphosphonium-4-tolyl)-20-(4-tolyl)-porphyrin; TPrPO, 2,7,12,17-tetra-*n*-propyl-porphycene; TrMPyP, 5,10,15-tris(*N*-methylpyridinium-4-yl)-20-(phenyl)porphyrin; TTP, 5,10,15,20-tetrakis(4-tolyl)porphyrin; UP, uroporphyrin I; VLDL, very low-density lipoproteins; ZnPc, zinc phthalocyanine; $ZnPc(OH)_4$, zinc tetrahydroxyphthalocyanine; ZnPcS, sulfonated zinc phthalocyanine; ZnTBP, zinc tetrabenzoporphyrin; ZnTDCSPP, zinc 5,10,15,20-tetrakis(2,6-dichloro-3-sulfonatophenyl)porphyrin; ZnTMPyP, zinc 5,10,15,20-tetrakis(*N*-methylpyridinium-4-yl)porphyrin; ZnTPPS, zinc 5,10,15,20-tetrakis(4-sulfonatophenyl)porphyrin

* Corresponding author. Tel.: +420-266-172-193; fax: +420-220-941-502.
E-mail address: lang@iic.cas.cz (K. Lang).

doi:10.1016/j.ccr.2004.02.004

Abstract

The binding of photosensitizers to host molecules is discussed from the perspective of how the confinement in a molecular assembly influences the sensitizer's photophysical properties. In connection with photodynamic therapy (PDT) of cancer during which the administered sensitizer necessarily interacts with the biological material the problem becomes of utmost importance. This review surveys changes of photophysical behaviour of porphyrins, metalloporphyrins and other porphyrinoid sensitizers induced by their interaction with biopolymers (proteins, nucleic acids), liposomes or synthetic sensitizer carriers (cyclodextrins, calixarenes). The structure, charge, and physicochemical properties of the sensitizer predetermine the type of interaction with the surrounding microenvironment and are manifested by changes in absorption, fluorescence, kinetics of deactivation of the excited states, and generation of singlet oxygen. As follows from the collected data, binding of the sensitizer does not restrict formation of the excited states but influences the kinetics. Various consequences of binding on the form and photophysical parameters of the sensitizers are discussed and general features of the mutual interaction are outlined.

Keywords: Non-covalent binding; Porphyrin; Excited states; Singlet oxygen; Photosensitizer; Biopolymers

1. Introduction

Photosensitized reactions of molecular oxygen have recently found far-reaching applications in biology and medicine. Complete understanding of these reactions in the complex biological environment became a topical interdisciplinary problem that spans from photophysics over photochemistry and photobiology to photomedicine [1–10]. The so-called photodynamic effect rests in the oxidative damage of biological material by reactive forms of oxygen generated by sensitized reactions. The photodynamically active species is singlet oxygen $^1O_2(^1\Delta_g)$ generated *in situ* by energy transfer from an excited sensitizer to oxygen molecule. Superoxide O_2^-, the product of electron transfer [1,2] is also involved, to a lesser extent. The photodynamic effect has been utilized, e.g., in photodynamic therapy (PDT) of cancer or atherosclerosis, in inactivation of some bacteria and viruses and in insecticides. The most intensively studied area is the photodynamic therapy of tumors. The treatment is based on administering the sensitizer usually by intravenous injections and, after a period necessary for retention of the sensitizer in the tumor, irradiation of the tumor by visible light. This way singlet oxygen and other reactive particles are formed directly in a tumor and destroy it from inside. Though numerous sensitizers produce singlet oxygen, almost all sensitizers studied in this context belong to the group of porphyrinoid ligands or their metallocomplexes. The collective term porphyrinoids denotes porphyrins and structurally similar macrocyclic compounds with four or more pyrrole rings.

The observed poor correlation between photophysical parameters of a sole sensitizer and its photodynamic efficacy turned attention to the influence of the biological environment. To be photodynamically active, the sensitizer needs to be closely associated with the target. Consequently, the favourable pattern of localization depends on the nature of the sensitizer (structural and physicochemical), nature of the sensitizer carrier, and on complex environmental conditions, which makes the final effect rather unpredictable. In chemical terms the influence of the environment can be attributed to non-covalent interactions of the sensitizer with surrounding molecules. Several papers have been dedicated to changes of photophysical parameters of sensitizers in the presence of proteins, nucleic acids, and some other molecules that may act as host molecules. It is worth noting the impact non-covalent interaction exerts on such intrinsic properties of the sensitizer molecule, as the photophysical quantities [3–6]. *Vice versa*, the change of photophysical properties can be a useful tool for getting information on the topology of binding sites and on the nature of interactions by which they were evoked. Our review of this developing area of chemistry is not intended to be exhaustive. Instead, it is intended to serve as a report highlighting photophysical characteristics of non-covalently bound sensitizers and the ways how knowledge of these characteristics can help in the prediction of photodynamic action caused by novel photosensitizers.

The interaction often affects the molecular form of the sensitizer, in most cases the equilibrium between monomeric and aggregated species. According to the charge and steric arrangement of either of the interacting components, the interaction can promote monomerization or support self-assembling into organized, often chiral, aggregates. Binding-induced aggregation is not a desirable process since photodynamic efficiency decreases as a result of the poor or absent sensitizing ability of dimers and higher aggregates [6,11]. In many respects, photodynamic effect bears upon self-assembling, formation of supramolecular structures and

molecular recognition and it may be inspiring to treat the problem from this point of view. Furthermore, time-resolved methods may fill in for the lack of information about the time course of processes.

The organization of the present review is as follows. The theoretical background of sensitization, singlet oxygen formation and specific requirements on suitable sensitizers are summarized in Sections 1.1. and 1.2. In Section 2 we review the photophysical properties of singlet oxygen producing porphyrinoid sensitizers[1] bound to well-defined molecules of biological importance. The photophysical characteristics including fluorescence quantum yields (Φ_f), quantum yields of the triplet states (Φ_T), quantum yields of the singlet oxygen formation (Φ_Δ), fluorescence (τ_f) and triplet (τ_T) lifetimes and rate constants of the triplet states quenching by oxygen (k_q) are summarized in Tables throughout the text. Figures documenting the described effects are taken from the authors' experiments. To the best of our knowledge, no attempt has been made at a direct comparison of the effect of binding on photophysical properties of porphyrinoid sensitizers. We believe that it can contribute to understanding and prediction of sensitizer behavior in the presence of biologically active compounds. Careful assessment of the binding effects and comparison of biopolymers and potential host molecules, such as cyclodextrins and calixarenes on the molecular level is a rational way to understand photosensitized processes in complicated biological environments. The future development of the topic is outlined in Section 3.

1.1. Photosensitized reactions of molecular oxygen

1.1.1. Energy and electron transfer

The oxygen molecule exhibits a series of absorption bands in the ultraviolet, visible and infrared. Although the direct photoexcitation of molecular oxygen [12] or oxygen–organic molecule charge transfer complexes [13] to produce singlet oxygen is possible, this method is not of much interest for preparative applications due to small yields of $^1O_2$. An indirect path of excitation, the photosensitized reaction (Scheme 1A), is therefore the core of photo-initiated reactions involving oxygen. Photosensitized oxygen reactions are classified as Type I and Type II according to the nature of a quencher [14] (Scheme 1B). Quenching of the excited sensitizer by molecular oxygen (Type II reactions) proceeds as energy transfer yielding singlet oxygen $^1O_2$ or as electron transfer yielding superoxide anion radical O_2^-. Energy transfer from the excited triplet state of the sensitizer to the ground state (triplet) oxygen is a spin allowed process, coupled with spin inversion of oxygen to two forms of singlet oxygen $^1O_2(^1\Delta_g)$ and $^1O_2(^1\Sigma_g)$ (Scheme 2)

$$^3\text{Sens}^* + {}^3O_2 \rightarrow {}^1\text{Sens} + {}^1O_2 \quad (1)$$

[1] Unless otherwise stated, the term sensitizer is synonymous with porphyrinoid compounds, both free ligands and metallocomplexes.

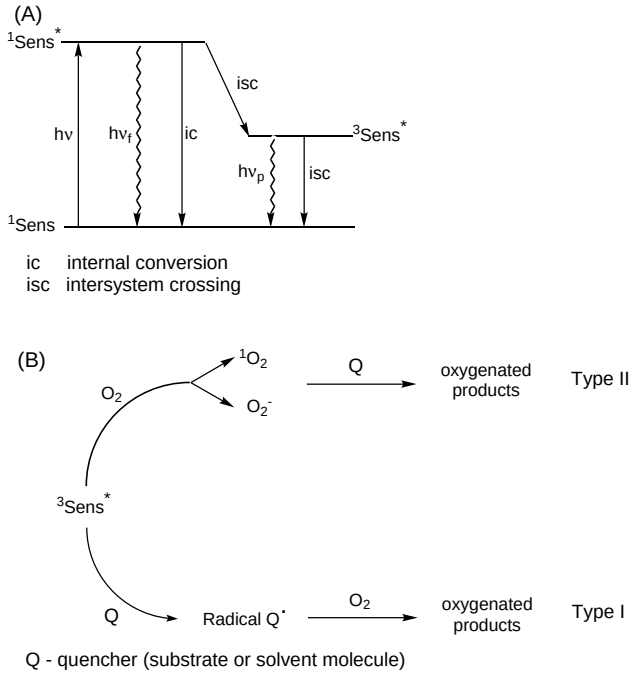

Scheme 1. Photosensitized singlet oxygen production (A) and reactions (B).

Occupation of the highest antibonding orbitals $2p\pi^*$ in the ground state and excited states is demonstrated in Scheme 2.

Electron transfer to oxygen generates doublet particles, a sensitizer cation radical and superoxide O_2^-

$$^3\text{Sens}^* + {}^3O_2 \rightarrow {}^3(^2\text{Sens}^+ \cdots {}^2O_2^-) \leftrightarrow {}^2\text{Sens}^+ + {}^2O_2^- \quad (2)$$

Quenching by substrate or solvent molecules yields the corresponding radicals (Type I reactions). The reactions producing O_2^- in the primary step (Eq. (2)) are of Type II—oxygen reactions [14,15], though they were originally described as Type I—radical reactions [9,16].

The excited singlet states S_1 of most sensitizers are too short-lived to be effectively quenched by oxygen and yield $^1O_2$. Nonetheless, singlet oxygen $^1O_2(^1\Delta_g)$ can be generated provided that the energy difference ΔE (S_1–T_1) of the sensitizer exceeds 94.1 kJ mol^{-1}. Singlet oxygen is generally accepted as a decisive species in the photodynamic action.

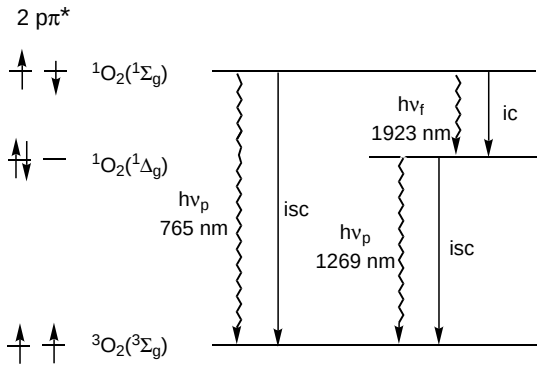

Scheme 2. Transitions between electronic states of oxygen in a solution.

Table 1
Properties of two lowest electronic states of singlet oxygen (full spectroscopic representation)

	$^1O_2$ ($a^1\Delta_g$)	$^1O_2$ ($b^1\Sigma_g^+$)	
Energy (kJ mol^{-1})	94.1		156.9
Transitions in solution (nm)	$^1O_2(a^1\Delta_g) \rightarrow {}^3O_2(X^3\Sigma_g^-)$ 1269–1282[a]	$^1O_2(b^1\Sigma_g^+) \rightarrow {}^3O_2(X^3\Sigma_g^-)$ 765[a]	$^1O_2$ ($b^1\Sigma_g^+$) → $^1O_2$ ($a^1\Delta_g$) 1914–1936[a]
τ_r (gas)[e]	64.6 min[a], 64 min[b]	11.8 s[a], 10 s[b]	6.7 min[b]
τ_r (solution)[e]	0.25–10 s[a]	1 s[a]	0.33–1.4 ms[a]
τ_Δ (H_2O)[f]	3.8 μs[c], 3.1–4.2 μs[d]	8.2 ps[a]	
τ_Δ (D_2O)[f]	62 μs[c], 55–68 μs[d]	42 ps[a]	

[a] [21].
[b] [26].
[c] [27].
[d] [28].
[e] Radiative lifetime.
[f] Natural lifetime.

The less frequently generated O_2^- is the parent species of $OH^\bullet$ radicals formed *via* dismutation of $O_2^-/HO_2^\bullet$ and the catalyzed Haber–Weiss reaction. As recent studies indicate, radical reactions of Type I and thermal processes connected with radiationless transitions of the excited sensitizer may also contribute to the final photodynamic effect [11,17,18].

In the absence of oxygen or any chemical reaction, the lifetime τ of an excited sensitizer is related to the rate constant of the monomolecular deactivation processes by

$$\tau_T = \frac{1}{k^T_{decay}} = \frac{1}{k_{phosphorescence} + k^T_{isc}} \quad (3)$$

for the triplet states, and

$$\tau_S = \frac{1}{k^S_{decay}} = \frac{1}{k_{fluorescence} + k_{ic} + k^S_{isc}} \quad (4)$$

for the singlet states (Scheme 1). In the presence of oxygen, the observed quenching rate of the triplet sensitizer is given by

$$k_{obs} = k^T_{decay} + k_q[O_2] \quad (5)$$

where k_q is the rate constant characterizing bimolecular quenching by oxygen and is expressed as the sum of oxygen dependent rate constants namely of energy transfer, electron transfer and enhanced intersystem crossing. Since diffusion controlled k_q is of the order of 10^9–10^{10} M^{-1} s^{-1}, the determination of the correct value of k^T_{decay} is extremely sensitive to traces of oxygen.

The quantum yield of singlet oxygen formation Φ_Δ depends on the quantum yield of the triplet states Φ_T according to

$$\Phi_\Delta = \Phi_T S_\Delta S_q \quad (6)$$

where S_Δ is the fraction of triplet molecules quenched by oxygen and yielding $^1O_2$ and is given by

$$S_\Delta = \frac{k_{et}}{k_q} \quad (7)$$

where k_{et} is the rate constant of energy transfer leading to the formation of $^1O_2(^1\Delta_g)$ and/or $^1O_2(^1\Sigma_g)$ (Scheme 2, Table 1), and S_q is the fraction of oxygen dependent triplet deactivations

$$S_q = k_q \frac{[O_2]}{k_q[O_2] + k^T_{decay}} \quad (8)$$

The denominator represents all pathways of triplet deactivations. If $k^T_{decay} \ll k_q[O_2]$, then $S_q \cong 1$ and for Φ_Δ holds the simplified equation [11,19]

$$\Phi_\Delta = \Phi_T S_\Delta \quad (9)$$

1.1.2. Singlet oxygen

In the context of photodynamic processes, the more stable $^1O_2(^1\Delta_g)$ form has been considered and monitored so far, and is referred to simply as "singlet oxygen". The growing interest in the formation and deactivation of $^1O_2(^1\Sigma_g)$ in a solution is motivated by an effort to acquire important information about the mechanism of photosensitized oxygen reactions and about solvent effects on forbidden radiative transitions [20,21]. Studies on $^1O_2(^1\Sigma_g)$ have been fostered by the development of sophisticated time-resolved spectroscopic methods [21–24].

Quenching of the sensitizers in the triplet states by oxygen in some organic solvents was shown to directly produce $^1O_2(^1\Sigma_g)$ and $^1O_2(^1\Delta_g)$ in the primary step of energy transfer [25].[2] The obvious stipulation is that the T_1 energies of the sensitizer must exceed the energy difference 157 kJ mol^{-1} between $^1O_2(^1\Sigma_g)$ and ground state oxygen. The branching ratios $^1\Sigma/^1\Delta$ depend on the nature of the sensitizer and the solvent and for the reported systems varied between 1.7 and 0.4. Apparently, a considerable fraction of $^1O_2(^1\Sigma_g)$ is generated in solution.

The energy level diagram and transitions between electronic states of oxygen are shown in Scheme 2. The competing processes of radiative and non-radiative decay of $^1O_2(^1\Sigma_g)$ and $^1O_2(^1\Delta_g)$ are solvent dependent because solvent perturbations enhance the probability of spin forbidden

[2] Formation of $^1O_2$ ($^1\Sigma_g$) by oxygen quenching of the sensitizers in the excited singlet states has not been experimentally confirmed.

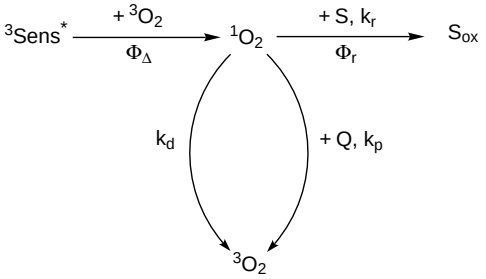

Scheme 3. Reactions of singlet oxygen.

transitions $^1\Sigma_g \rightarrow {}^3\Sigma_g$ and $^1\Delta_g \rightarrow {}^3\Sigma_g$. The rate constants of radiative decay of $^1O_2(^1\Sigma_g)$ and $^1O_2(^1\Delta_g)$ in a solution are significantly lower than are those of non-radiative processes. Hence, it is the non-radiative decay that prevails in solutions. With respect to deactivation, the spin allowed path $^1O_2(^1\Sigma_g) \rightarrow {}^1O_2(^1\Delta_g)$ is dominant with almost unit efficiency. The viability of the path is supported by the fact that a lesser amount of energy $\Delta E = 62.8\,\mathrm{kJ\,mol^{-1}}$ needs to be dissipated. It follows that $^1O_2(^1\Delta_g)$ originates from oxygen quenching of triplet sensitizer through two reaction paths—one direct, the other indirect via $^1O_2(^1\Sigma_g)$ [21,25]. Speculation that $^1O_2(^1\Sigma_g)$ can participate in photosensitized oxidation have not been confirmed [25]. This justifies the general belief that $^1O_2(^1\Delta_g)$ is the decisive oxidation agent in photodynamic processes. The relevance of $^1O_2(^1\Sigma_g)$ for photodynamic processes rests in the fact that it can be a precursor of $^1O_2(^1\Delta_g)$ since practically all $^1O_2(^1\Sigma_g)$ decays to $^1O_2(^1\Delta_g)$ [25]. Some of the characteristics of both forms of $^1O_2$ are summarized in Table 1.

Singlet oxygen can be consumed in two competing ways: (i) physical quenching of $^1O_2$ by a quencher that becomes electronically excited (bimolecular) or deactivation proceeding by vibrational excitation of solvent molecules (monomolecular). (ii) Oxidation of a molecule by $^1O_2$ (chemical reaction). Quenching and oxidation of substrates in the ground singlet state are spin allowed reactions. The mechanism of singlet oxygen reactions—solvent deactivation and reactions with quenchers and substrates—are visualized in Scheme 3.

The fraction of $^1O_2$ molecules that react with the substrate S to oxidized substrate S_{ox} is

$$f_r = \frac{k_r[S]}{k_r[S] + k_d + k_p[Q]} \tag{10}$$

where k_r is the rate constant of oxidation reaction, k_p the rate constant of physical quenching by a quencher Q, and k_d the rate constant of deactivation in the absence of S and Q. If no quencher is present, the quantum yield of the oxidized substrate Φ_r is given by

$$\Phi_r = \Phi_\Delta f_r = \Phi_\Delta \frac{k_r[S]}{k_r[S] + k_d} \tag{11}$$

Clearly, when $k_r[S] \gg k_d$, the above equation simplifies to $\Phi_r = \Phi_\Delta$; in this case entire $^1O_2$ produced is consumed in a reaction with the substrate (saturation effect) [29].

Due to the high reactivity of $^1O_2$ with substrates, the chemistry of $^1O_2$ is very rich [19,29–31]. Still, the reactions have certain selective features. Typical reactions involving C=C bonds, isolated or conjugated, are oxidations of olefins (ene-type reactions, [2+2] cycloadditions), 1,3-dienes ([4+2] cycloadditions), aromatic compounds and heterocycles. The intermediates are peroxo species, such as perepoxides, dioxethanes and endoperoxides. Thiocompounds are oxidized to sulfoxides, and phosphines to phosphine oxides [29]. In the context of this review singlet oxygen reactions with constituents of proteins, lipids and DNA are relevant.

Amino acids (amino acid residues in proteins). Among essential amino acids the most prone to oxidation with $^1O_2$ are cysteine, methionine, histidine, and tryptophan [26,29,32]. Due to their reactivity, these amino acids are the primary target of an oxidative attack on proteins. The reaction mechanisms are rather complex and as a rule lead to a number of final products. Cysteine and methionine are oxidized mainly to sulfoxides, histidine yields a thermally unstable endoperoxide, tryptophan reacts by a complicated mechanism to give *N*-formylkynurenine.

Lipids. Unsaturated lipids typically undergo ene-type reactions [33].

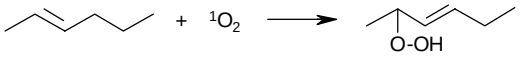

(12)

DNA. Of the four nucleobases guanine is the most susceptible to oxidation by $^1O_2$. The reaction mechanism has been extensively studied in connection with oxidative cleavage of DNA [34–36]. The first step is a [4 + 2] cycloaddition to the C-4 and C-8 carbons of the purine ring leading to an unstable endoperoxide. The subsequent complicated sequence of reactions and the final products depend on whether the guanine moiety is bound in an oligonucleotide or a double-stranded DNA [37].

Generally, the reactions of $^1O_2$ are sensitive to steric factors. A novel approach pays special attention to the effects of the environment namely to the ability of supramolecular structures to control conformation of the built-in substrates and/or sensitizers. This approach is expected to yield relevant information on reactions proceeding in biological systems on the cellular level. The supramolecular structures can be composed of micelles, cyclodextrins, zeolites, calixarenes, etc. Recently, the effects of micelles, cyclodextrins or synthetic membranes as host structures on singlet oxygen reactions were reviewed [31].

1.2. Sensitizers

Numerous sensitizers produce singlet oxygen and can be considered suitable for PDT, nevertheless, the majority

of sensitizers investigated in this context were compounds with a porphyrinoid structure [7–10,33]. The reason for this preference is the extensive knowledge of their chemistry together with the inherent similarity to natural porphyrins frequently occurring in living matter. Of non-porphyrinoid sensitizers eosine, acridine, rose bengal, methylene blue, perylenequinones, triarylmethane dyes, etc. have been taken into consideration. The effort to correlate the structure of the sensitizer to intermolecular non-covalent interactions produced a categorical requirement to use well-defined individual sensitizers. Mixtures of derivatives, species differing in the number of substituents or even different regioisomers, interacting differently with biomolecules in the tissue, often yield misleading results on structure–activity relationships [7,33].

Sensitizers suitable for PDT have to meet a number of specific requirements:

- *Maximum absorption in the region 600–800 nm* [7,33,38]. The incident intensity of light—irradiance—is reduced by absorption by chromophores in tissue or by scattering. The efficiency of scattering increases as the wavelength is decreased. On the other side, absorption by water molecules increases at wavelengths above 800 nm. Consequently, the window for optimum penetration lies between 600 and 800 nm, i.e. in the region of red light. The characteristic quantity is the penetration depth δ defined as the depth in which the irradiance is reduced to $1/e$ of the initial value. Typical values of δ vary between 1 and 3 mm, but apparently the photodynamic effect reaches beyond this limit. The upper limit of the wavelength to produce $^1O_2$ is given by the energy necessary for the $^1O_2$ formation ($\lambda < 1269$ nm, $\Delta E > 94.1$ kJ mol^{-1} for a one-photon process).
- *Minimum absorption in the region 400–600 nm* [11,39,40]. Sensitizers absorbing in this region, i.e. in the maximum of the spectroscopic distribution of daylight, enhance photosensitivity of the skin, which is a complicating side effect of photodynamic treatment. Photosensitization of skin has been the major drawback of first generation sensitizers based on hematoporphyrin derivatives.
- *High quantum yields of* $^1O_2$. The quantum yields Φ_Δ vary in the range 0.3–0.8 for most sensitizers. The significance of Φ_Δ should not be overestimated, since the amount of $^1O_2$ produced depends strongly on other factors, namely on interaction of the sensitizer with surrounding biopolymers, aggregation of the sensitizer, oxygen depletion and side reactions. The demand of high Φ_Δ includes the prerequisite of adequately high Φ_T, the triplet state energy sufficient for the $^1O_2$ formation and relatively long lifetime of the triplet states τ_T.
- *Photostability*. A sensitizer should be stable against photodegradation and against oxidation by $^1O_2$ or other reactive oxygen species generated *in situ*. Photobleaching of sensitizers in biological systems is a complex process, not necessarily oxygen dependent. Photobleaching plays an important role in decreasing skin sensitization and the specificity of phototreatment [7,8,40,41].
- *Non-toxicity and phototoxicity*. Low "dark" toxicity (e.g. nephrotoxicity, neurotoxicity) is desirable so as to avoid unnecessary strain on the organism prior to irradiation. The overall destructive photodynamic effect of the sensitizer on biological material *in vitro* or *in vivo* is called phototoxicity.
- *Specific retention in the malignant tissue*. The specific retention of a sensitizer in the malignant tissue is a consequence of different kinetics of sensitizer removal from the malignant and healthy tissue. The removal from the healthy tissue is faster. The concentration difference is adjusted within several hours after sensitizer administration and depends on the nature of the sensitizer. Effectual removal of the sensitizer from the healthy tissue precludes its photodynamic damage [4].
- *Single substance*. The use of a single, well-defined substance is necessary for reliable evaluation of the sensitizer–biopolymer interaction [7,33].
- *Fluorescence*. Fluorescence of the sensitizer enables detection of the sensitizer distribution *in vivo*. To retain both functions of the sensitizer, namely fluorescence and $^1O_2$ production, the ratio Φ_f/Φ_{isc} should be optimised [11].
- *Solubility*. Sufficient solubility of the sensitizer in aqueous media is important for direct intravenous application and transport to the intended target location. Hydrophobic, insoluble sensitizers can be transported by water-soluble carriers [17,31,42]. The role of possible carriers will be discussed in Section 2.

It is not the intention of this review to provide an exhaustive description of the numerous porphyrinoid sensitizers applicable in PDT. Several excellent reviews exist [7–10,33,43–46]. Basic skeletons are presented in Scheme 4. Structures **1**–**4** were originally natural products, whose synthetic analogues are used as a rule. Synthetic porphyrins **1** are often substituted in the *meso*-positions. Chlorin **2** and bacteriochlorin **3** are partly hydrogenated porphyrins; hydrogenation shifts the absorption bands to the more advantageous region above 600 nm. Purpurins **4** are degradation products of chlorophylls. Compounds **5**–**12** are purely synthetic and have no counterpart in nature. Porphyrazine or tetraazaporphyrin **5** is the basic skeleton of the extensively used phthalocyanines **6** and naphthalocyanines **7** [47]. Among novel types of porphyrinoid compounds **8**–**12** are new sensitizers, some of which are very promising for PDT. Porphycenes **8** are isomeric porphyrins with differing length of the pyrrole–pyrrole bridges [48,49]. Expanded porphyrins **9** are characterized by an increased number of atoms separating the pyrrole rings. The most important expanded porphyrins are sapphyrins **10** and texaphyrins **11** [9,43,50]. A trend opposite to expansion of the macrocycle follow subphthalocyanines **12** with three diiminoisoindole rings bound to a central boron atom [51]. Generally, porphyrinoid sensitizers can be free ligands or metallocomplexes with Al,

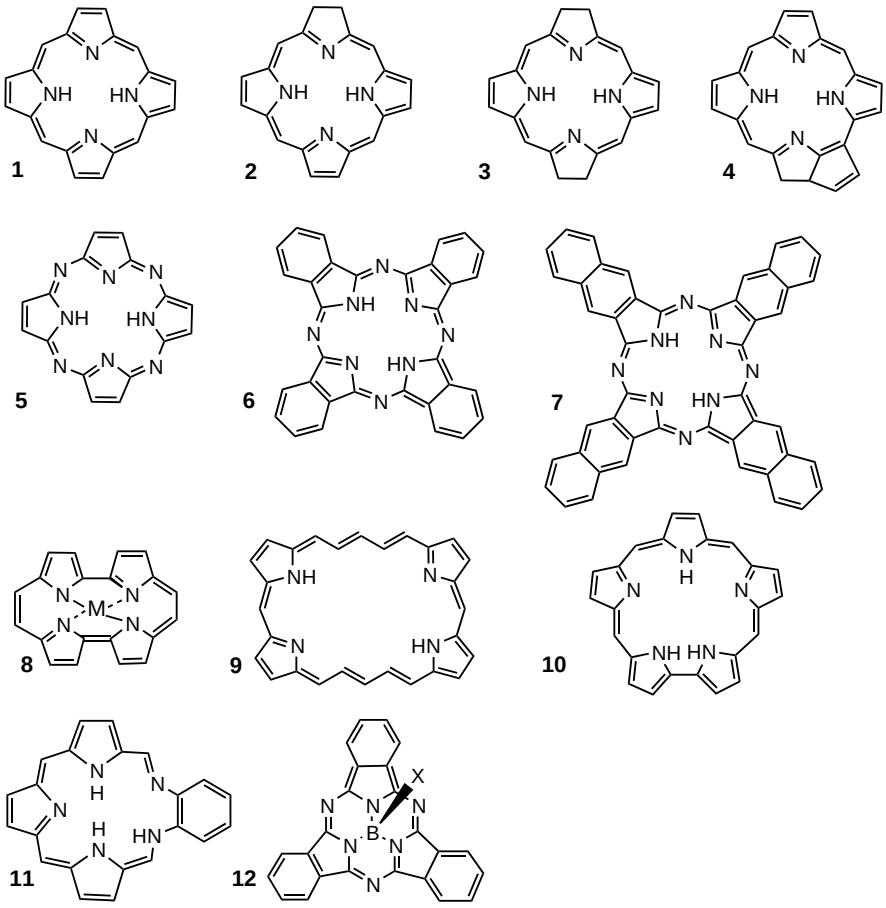

Scheme 4. Basic structures of porphyrinoid sensitizers.

Zn, Mg, Ga, Si, Ge, Sn, or lanthanides [9,33,43,48,49] central ions. *Meso*-substituted porphyrins, chlorins and some expanded porphyrins are usually applied as free ligands (non-metallated). On the other hand, phthalocyanines and naphthalocyanines are always metallated since the free ligand is less chemically stable [7]. Complexes with transition metals are poor sensitizers because of their short triplet lifetimes ranging from picoseconds to nanoseconds.

The following paragraphs review the principal types of sensitizer arranged according to the charge of the peripheral groups. The charge, its sign and distribution, and hydrophilicity or hydrophobicity of the sensitizer predestine the mode of interaction with biomolecules and/or carriers and, consequently, photophysical properties, the fate, and effectiveness of the sensitizer in a biological system. The tetrapyrrolic sensitizers, anionic or cationic, with three or four charged substituents are hydrophilic (polar). Monosubstituted and disubstituted sensitizers behave as amphiphilic molecules (vide infra). Symmetric disubstitued sensitizers have more hydrophilic character than the asymmetric [8,33].

Of the anionic sensitizers sulfonated or carboxylated metallophthalocyanines and *meso*-tetraphenylporphyrins have been most frequently investigated. *In vitro* and *in vivo* studies have been carried out in order to map a correlation between sulfonation degree and photodynamic activity [4,7,8,11,33,52]. Anionic sensitizers interact with proteins possessing positively charged side chains—protonated amino nitrogen atoms. Highly basic proteins can compensate repulsion between the negatively charged sensitizer molecules and promote aggregation of the sensitizer [53]. The observation that the cationic sensitizer TMPyP intercalates into DNA at the G–C base pairs [54] and the capacity to penetrate into the nucleus [55] gave impetus to extensive studies of novel cationic sensitizers. The positive charge is usually localized on the protonated pyrrole nitrogen atoms (e.g. sapphyrins) and the quaternized pyridinium or ammonium nitrogen. The cationic sensitizers are less numerous than the anionic. Besides the most widely used TMPyP [55] cationic tetratolylporphyrins [56,57], pyridinoporphyrazines [47,58], and pyridinium or trimethylammonium phthalocyanines [59,60] have also been investigated.

The class of hydrophobic sensitizers involves a number of uncharged species among which phthalocyanines and naphthalocyanines prevail over porphyrins and porphycenes. The advantage of hydrophobic sensitizers in PDT lies in their affinity to lipid membranes. Axial ligands, such as cholesterol coordinated to central ions of phthalocyanines and naphthalocyanines or apolar peripheral substituents

(carotenoid chain, butoxy groups) can be used to enhance the hydrophobicity/lipophilicity of the sensitizer and hence its uptake by the cells. Due to the insolubility of the hydrophobic sensitizers, a suitable carrier (lipid emulsion, liposomes, micelles, cyclodextrins) is to be used for their administration [6,7].

The amphiphilic sensitizers possess separated hydrophilic and hydrophobic regions that can independently interact with other adjacent molecules [7]. The amphiphilic sensitizers are photodynamically more active than symmetric hydrophilic or hydrophobic sensitizers [8]. The activity is not necessarily correlated with photophysical properties of the isolated molecule in solution. Systematic studies of variously sulfonated Al phthalocyanines $AlPcS_n$ and tetraphenylporphyrins ($1 \leq n \leq 4$, n is the number of the sulfonato groups) as model sensitizers have unambiguously shown maximal activity of unsymmetrical disulfonated compounds. Important amphiphilic sensitizers, confirming good prospects for this class in PDT, are 5,10,15,20-tetrakis(*m*-hydroxyphenyl)chlorin (THPC) and benzoporphyrin derivatives (verteporphin) [7,9,33].

The approximately planar porphyrinoid sensitizers tend to form stacked dimers and higher aggregates in polar solvents, held together by π–π interactions of the aromatic rings and by hydrophobic interactions. As it is known from experimental observation, aggregated sensitizers produce very little $^1O_2$ and have low, if any, photodynamic activity [6,11]. Dis-aggregation as a consequence of interaction between the sensitizer and biopolymers (proteins, DNA) will be discussed in the following sections.

2. Non-covalent interactions

In this section, we present brief introduction to the types of non-covalent interactions that are responsible for molecular assembling. By non-covalent interactions are understood weak binding forces, by whose action assemblies of molecules arise, but not new molecules, as with a chemical reaction. Interactions govern the structure and stability of assemblies, and play a decisive role in molecular recognition.

The common features of non-covalent interactions are the distinctly lower bond energies than those of the covalent bonds. Whereas typical ΔH values of a simple covalent bond range from 150 to 500 kJ mol^{-1}, ΔH of non-covalent interactions is as a rule <100 kJ mol^{-1}, the weakest being of the order of units kJ mol^{-1}. Usually, molecular association is made possible not by a single weak interaction but through the simultaneous cooperation of several weak interactions. The interactions form two distinct groups—hydrophobic interactions and electronic interactions. The latter group involves hydrogen bonds, Coulombic interactions, π interactions, charge-transfer interactions, and dispersion forces. Characteristic properties of interactions most important for the formation of assemblies are [61,62]: (i) Directionality—orientation of the bond in the space or towards a certain atom or group affects specificity of the interaction. (ii) Range of the intermolecular forces—is proportional to $1/r^m$, where r is the distance and m the integer $1 \leq m \leq 6$. (iii) Strength of the bond.

Hydrogen bond (typically O–H···O) is the most common type of interaction and can be described as interaction between a proton donating group, such as OH, NH, CH and a proton acceptor (F, O, N, Cl, Br, I) [62,63]. The strength of the bond depends on the electronegativities of both atoms bridged by the proton. The bonding enthalpies, usually in the range of 12–120 kJ mol^{-1}, reflect the diversity of this type of interaction. Hydrogen bonding is strictly directional and selective, which means, that it has a determinative structural effect. Hydrogen bonding occurs in aqueous and non-aqueous media.

Coulombic (electrostatic) interactions are caused by attraction or repulsion between static molecular charges, ions, permanent dipoles or quadrupoles in any combination of the pair. Electrostatic interactions in principle also include hydrogen bonding that may be considered a special case of electrostatic attraction. The interaction is directional and short range. An example of electrostatic interaction is binding of anionic dyes to albumin [64,65].

Interactions involving π electrons represent an important group of non-covalent interactions, essentially different from electrostatic interaction. The π interactions include π–π interactions, cation–π interactions and CH–π interactions. The interaction of the π clouds can be either attractive or repulsive, according to the mutual orientation of the aromatic rings. Whereas the direct face-to-face orientation is repulsive, the edge-to-face, T-shaped or stacked (shifted) arrangements are attractive. The last mentioned arrangement has an important organising effect on vertical building of helical structures in biopolymers [66]. The π–π interactions are less directional and weaker than hydrogen bonding, and distinctly long range [67]. The cation–π interaction is a relatively strong, short-distance interaction between an organic or inorganic (e.g. alkali metal) cation and a molecule containing π-bonds, not necessarily aromatic, with a substantial electrostatic contribution. It is acting especially in aqueous media and by means of binding solvated cations it can compete with hydrophobic interactions between aromatic rings [68]. The CH–π is a very weak interaction with the bond enthalpy $\Delta H \geq 4$ kJ mol^{-1}. The importance of such weak interactions lies in the multiplication effect of numerous CH groups of large organic molecules, able to interact with the aromatic π system. The CH–π interactions participate, for instance, in complexation of aromatic compounds within the cavity of cyclodextrins [61,62].

Dispersion interactions, sometimes denoted as London or van der Waals forces, are of quantum origin and arise from interaction between fluctuating electron cloud of a molecule and temporary dipoles induced in the environment. Dispersion forces have typically low directionality and decrease with $1/r^6$. Due to these properties they have predominantly a stabilizing effect on molecular assemblies and biopolymers,

whereas the structure is directed by electrostatic or by π–π interactions [67,69].

Hydrophobic interactions differ from other non-covalent interactions by their non-electronic nature and absence of directionality and specificity. Hydrophobic interactions are caused by the tendency of hydrophobic regions to minimize the area of contact with a polar solvent by association of non-polar regions of two molecules and are primarily connected with aqueous media. The interaction is associated with a small enthalpy change ($\Delta H = 0.8$–$2\,\mathrm{kJ\,mol^{-1}}$), so that it is driven by entropy effects. Hydrophobic forces are responsible for, e.g., the tertiary structures of proteins, association of non-polar molecules with proteins and formation of inclusion complexes [61,62,67].

In addition to non-covalent interactions *coordination bonds* can also play an important role in molecular assembling and recognition. Planar metalloporphyrins with accessible axial ligands can act as templates and by coordination of molecules exert a directional effect on building of supramolecular structures [70]. Typical examples are zinc porphyrins [71,72].

2.1. Interaction with biopolymers

Porphyrinoid sensitizers form a number of complexes with biopolymers non-covalently bound by forces of electronic and hydrophobic nature. The non-covalent complexation changes, among others, the photophysical properties because the sensitizer molecule feels a different environment, usually less polar than in aqueous media, and because its internal movements are restricted. In addition, solvation dynamics in many supramolecular assemblies is slower than that in bulk water by two to four orders of magnitude indicating that the highly constrained water molecules can control reactivity and dynamics of supramolecular systems [73]. The assessment of the effects evoked by complexation with proteins, nucleic acids, liposomes or carriers, such as cyclodextrins or calixarenes can open new ways to improvement of solubility, enhancement of chemical or photochemical stability, and increase of the efficiency of photosensitization. In biological systems the efficiency of the photodynamic process depends on the sensitizer localization in cells and subcellular compartments. Photophysical properties of the monomeric or aggregated form of the bound sensitizers are important. Maximal effect is attained when the sensitizer is monomeric and becomes closely associated with the molecule that is intended as the target of the oxidative attack. Close association is necessary due to the short diffusion path of $^1O_2$ and other cytotoxic species during their life span.

The following paragraphs pertain to photophysical properties of porphyrinoid sensitizers non-covalently bound to well-defined molecules of biological importance namely proteins and nucleic acids. Photophysical properties—fluorescence, triplet state quantum yields and lifetimes, singlet oxygen formation—are essential for subsequent reactions of electronically excited sensitizers with target molecules (Type I reactions) or with dissolved oxygen (Type II reactions) (Scheme 1). Photosensitized oxidations are mostly mediated by the first triplet states (Scheme 1) because the triplet states live much longer than do corresponding singlet states. For this reason the triplet lifetimes, Φ_T and Φ_Δ will be emphasized in particular. Data collected for different types of non-covalent complexes with target molecules can bring new information on the porphyrinoid binding sites and on photosensitization effects in biological systems. It would be desirable to establish a correlation between the binding mode and change induced in the photophysical properties. The molecular structures of currently studied sensitizers together with corresponding abbreviations used throughout this review are presented in Scheme 5.

2.1.1. Nucleic acids

Water-soluble porphyrin sensitizers[3] bound to nucleic acids have been an object of numerous studies in connection with their antiviral activity [74], high photocleavage efficiency [36], nuclease activity [75], specific detection of DNA structures [76] and delivery vehicles for antisense oligodeoxynucleotides [77].

Three binding modes have been distinguished for the interaction of cationic porphyrins with DNA: (i) intercalation, (ii) outside groove binding, and (iii) outside binding with porphyrin self-stacking [54,78–81]. The last mode leads to the formation of organized porphyrin structures on the DNA exterior. Porphyrin derivatives, depending on their structure, central metal and axial ligands prefer not only a particular binding mode, but also certain DNA sequences. The binding modes and sequence preferences have been investigated using a wide variety of techniques, such as X-ray crystallography, UV-Vis, CD, fluorescence, NMR spectroscopy and resonance light-scattering experiments. It was found, for example, that cationic TMPyP and its metallocomplexes (e.g. Cu^{II}, Pd^{II}, Pt^{II}) possess appropriate properties as positive charge, size and planar geometry favorable for intercalation between guanine/cytosine base pairs (GC) of double-stranded DNA. More sterically demanding porphyrins—TMPyP metallocomplexes (ZnTMPyP, MnTMPyP or CoTMPyP) with axial ligands, or porphyrins with bulky *meso*-substituents (e.g. tetratolylporphyrin derivatives) [56,57,82]—are bound to the DNA surface with a preference for adenine/thymine base pair (AT) rich sequences. Recently, it was shown that one of the most important factors directing the binding mode is the local rigidity of the DNA duplex [81,83]. Therefore, nucleic acids that include at least 50% GC base pairs can support intercalative binding with or without contiguous GC base pairs in the sequence because a robust framework of hydrogen bonding stabilizes the intercalated adduct and inhibits structural distortions that support external binding.

[3] Only the photophysical properties of porphyrins bound to nucleic acids are described in literature.

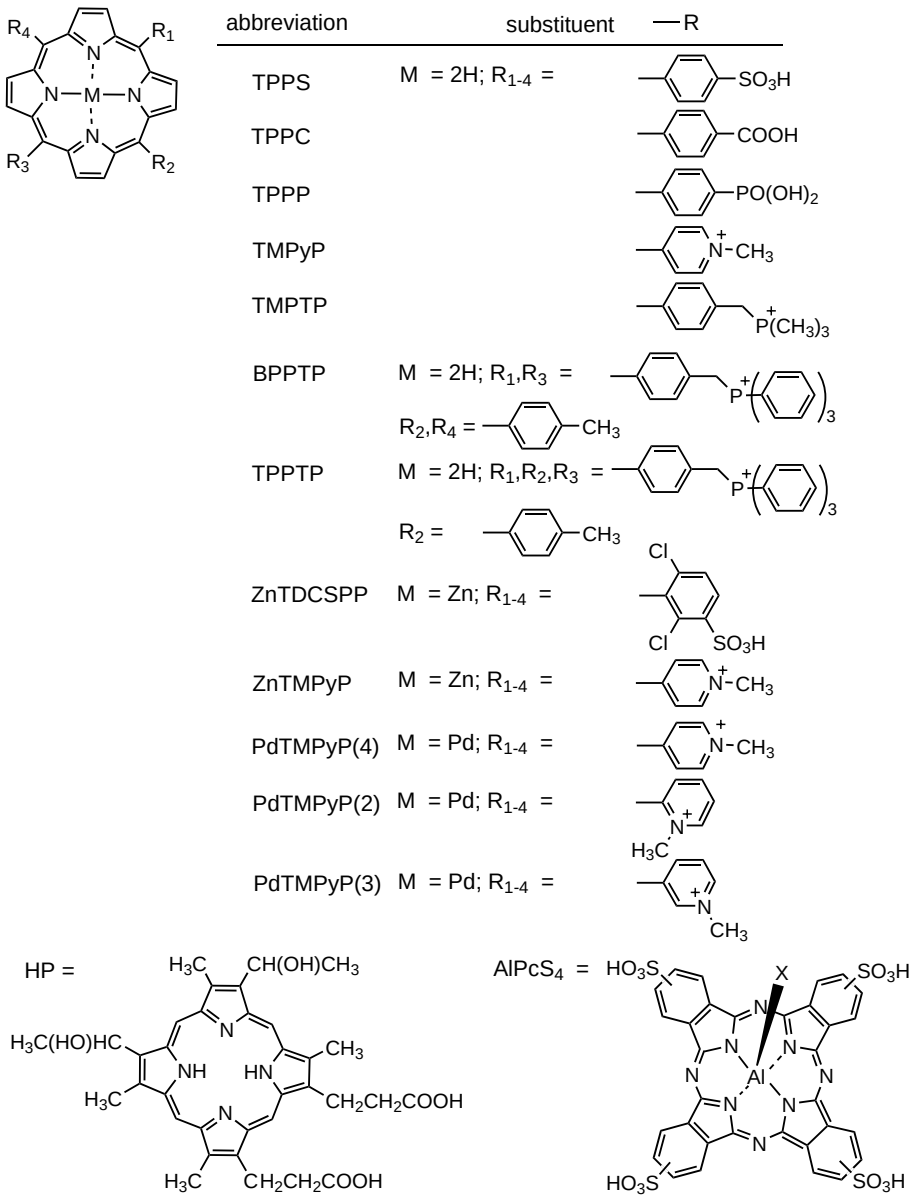

Scheme 5. Molecular structures of some sensitizers including abbreviations used throughout the text.

The formation of reversible exciplexes with nucleic acids [84] and reported photocleavage efficiency [36] depend on the photophysical characteristics of the bound porphyrins [56,57,82,85–88]. The importance of the porphyrin charge is evident from comparison of cationic TMPyP and anionic TPPS. Because electrostatic repulsion between the sulfates of TPPS and the backbone phosphates does not allow binding to the duplex the triplet and excited singlet states of TPPS are not affected at all [89]. On the contrary, the photophysics of TMPyP bound to DNA differs considerably.

This section pursues photophysical characteristics of porphyrins that are either intercalated or bound externally as monomers on nucleic acids (Tables 2 and 3). To specify the photophysical characteristics in individual binding modes, steady-state and time-resolved spectroscopic studies have to be carried out at low porphyrin concentrations. If the porphyrin is predominantly monomeric in solution, and if the porphyrin/DNA molar concentration ratios (DNA concentration given in base pairs) are less than 0.05 (ionic strength <0.1), the equilibrium concentration of unbound porphyrin is minimized because porphyrin either intercalates between base pairs or binds to the DNA exterior. Self-stacking on the DNA backbone is suppressed. But if porphyrin is more hydrophobic or a solution has higher ionic strength, then porphyrin aggregates formed directly in the solution deposit readily on the surface of nucleic acids without changing their structure and size [57].

Porphyrin self-stacking or porphyrin aggregation on the nucleic acid exterior, described above as the third binding mode, leads to the fast dissipation of absorbed energy me-

Table 2
The photophysical characteristics of porphyrins bound to nucleic acids in aqueous solution: fluorescence quantum yields (Φ_f), fluorescence lifetimes (τ_f), triplet lifetimes in deoxygenated aqueous solutions (τ_T), triplet lifetimes in air-saturated aqueous solutions (τ) (2.8×10^{-4} mol dm^{-3} O_2 at 25 °C under normal atmospheric pressure), and rate constants of the triplet states quenching by oxygen (k_q)

Complex	Φ_f	τ_f (ns)	τ_T (μs)	τ (μs)	$k_q \times 10^{-9}$ (M^{-1} s^{-1})	Mode
TMPyP	0.044[c]	4.6[c], 5.29[h] 4.9[k]	150[b], 170[c] 160[k]	2[i], 1.9[b] 1.8[k]	1.86[i], 1.9[b] 2.0[k]	–
TMPyP/dAMP[h]	–	11.3	–	–	–	–
TMPyP/dTMP[h]	–	10.3	–	–	–	–
TMPyP/dCMP[h]	–	7.8	–	–	–	–
TMPyP/dGMP[h]	–	0.69, 3.0	–	–	–	–
TMPyP/[poly(dG-dC)]$_2$	0.027[c]	2.5[c], 7.0[c]	1700[b], 1300[c]	30.0[i], 23.7[b]	0.12[i], 0.15[b]	A
TMPyP/[poly(dA-dT)]$_2$	0.085[c]	12.0[c]	800[b], 1600[c]	5.5[i], 20.5[i] 4.6[b], 18.8[b]	0.68[i], 0.18[i] 0.78[b], 0.19[b]	B
TMPyP/DNA[a]	0.041[c]	2.5[c], 11.0[c] 1.7[g], 10[g]	600[d], 470[c]	4.5[i], 18.0[i] 3.0[d], 18.1[d], 25.7[d]	0.83[i], 0.20[i] 1.2[d], 0.20[d], 0.14[d]	A, B
TMPyP/[d(TACGTA)]$_2$[f]	0.029	3.2, 8.0	–	7.0, 29.0	0.5, 0.12	A, B
TMPyP/[d(TAGCTA)]$_2$[f]	0.021	2.7, 10.4	–	6.0, 26.5	0.6, 0.14	A, B
ZnTMPyP[g]	–	1.3	–	–	–	–
ZnTMPyP/DNA[g]	–	1.8	–	–	–	B
PdTMPyP(2)[e]	–	–	105	2.2	1.6	–
PdTMPyP(2)/DNA[a,e]	–	–	125	8.0	0.4	B
PdTMPyP(2)/[poly(dG-dC)]$_2$[e]	–	–	–	8.1	0.4	B
PdTMPyP(3)[e]	–	–	100	3.0	1.2	–
PdTMPyP(3)/DNA[a,e]	–	–	360	63.1	0.06	A
PdTMPyP(3)/[poly(dG-dC)]$_2$[e]	–	–	–	47.2	0.08	A
PdTMPyP(4)[e]	–	–	115	1.6	2.2	–
PdTMPyP(4)/DNA[a,e]	–	–	350	36.2	0.1	A
PdTMPyP(4)/[poly(dG-dC)]$_2$[e]	–	–	–	48.0	0.07	A
TMPTP[j]	0.051	–	–	1.7	2.1	–
TMPTP/d(C_8)[j]	0.047	–	–	–	–	–
TMPTP/d(G_8)d(C_8)[j]	–	–	–	10.3	0.35	B
TMPTP/d(G_{16})d(C_{16})[j]	0.046	–	–	14.7	0.24	B
TMPTP/d(T_8)[j]	0.044	–	–	13.2	0.27	–
TMPTP/d(A_8)d(T_8)[j]	0.047	–	–	12.7	0.28	B
TMPTP/d(A_{16})d(T_{16})[j]	–	–	–	13.5	0.26	B
TMPTP/DNA[a,j]	0.036	–	–	13.9	0.26	B

The dominant binding modes reported for summarized complexes are intercalation (A) or outside groove binding (B).
[a] *Calf thymus* DNA, double-stranded, phosphate buffer, pH ∼ 7.
[b] [82].
[c] [85].
[d] [89].
[e] [88].
[f] [86].
[g] [92], chicken blood erythrocytes DNA, phosphate buffer pH 7.
[h] [95].
[i] [87].
[j] [57].
[k] [94].

diated by exciton coupling between the stacked porphyrin units. This mode considerably reduces fluorescence lifetimes and quantum yields, and suppresses formation of the porphyrin triplet states and of $^1O_2$ [56,57,82,90]. From the standpoint of the formation of $^1O_2$, only monomeric species and possibly planar end-to-end aggregates are endowed with significant photosensitizing ability [6]. Because many cationic porphyrins tend to aggregate in aqueous solutions, most literature data deal with the photophysics of TMPyP and its metalloderivatives, which stay predominantly monomeric. Also TMPTP appears to be a suitable sensitizer as reported recently [57].

Localization of *N*-methylpyridinium porphyrins within the duplex of DNA, [poly(dG-dC)]$_2$ or [poly(dA-dT)]$_2$, i.e. intercalation between GC base pairs or external groove binding, has a remarkable impact on its electronic absorption spectrum especially in the Soret region (ca. 400–450 nm). This band corresponds to excitation to the S_2 states with a high transition moment. Large red shifts of the porphyrin Soret maximum (≥15 nm) and a substantial hypochromicity of the Soret band (≥35%) of intercalated porphyrin complexes are due to close π stacking between the porphyrin molecule and GC base pairs that are the binding site of a high local rigidity [79] (Fig. 1c). The sequences rich in AT base pairs are relatively flexible because they have only two hydrogen bonds between bases. This allows only a limited amount of π stacking between the porphyrin molecule and one or more bases and, hence, better accessibility of

Table 3
Quantum yields of the triplet states (Φ_T), quantum yields of the singlet oxygen formation (Φ_Δ) and the fraction of the triplet states quenched by oxygen (S_Δ) of porphyrins bound to nucleic acids in D_2O

Porphyrin	Φ_T	Φ_Δ	S_Δ	Mode
TMPyP	0.85[b]	0.9[c], 0.74[g]	1.0[c]	–
TMPyP/[poly(dG-dC)]$_2$	0.44[b]	0.47[c]	1.0[c]	A
TMPyP/[poly(dA-dT)]$_2$	0.95[b]	0.71[c]	0.75[c]	B
TMPyP/DNA[a]	0.77[b]	0.57[c]	0.74[c]	A, B
TMPyP/[d(TACGTA)]$_2$	0.47[d]	–	–	A, B
TMPyP/[d(TAGCTA)]$_2$	0.54[d]	–	–	A, B
PdTMPyP(2,3,4)	1.00[e]	0.80[f]	–	–
PdTMPyP(2,3,4)/DNA	–	0.80[f]	–	A, B

The dominant binding modes are intercalation (A) or outside groove binding (B).
[a] *Calf thymus* DNA, double-stranded.
[b] [85].
[c] [87].
[d] [86].
[e] [97].
[f] [88].
[g] [98], H_2O as a solvent.

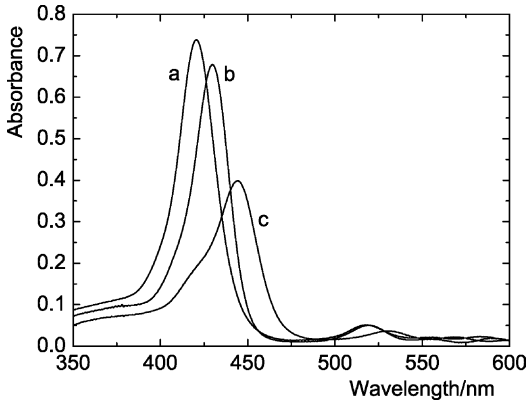

Fig. 1. Absorption spectra of 3.3 μM TMPyP in phosphate buffer (a), externally bound TMPyP on [poly(dA-dT)]$_2$ (b) and intercalated TMPyP in [poly(dG-dC)]$_2$ (c). Air-saturated 20 mM phosphate buffer, 100 mM NaCl, pH 6.9, porphyrin/DNA (in base pairs) molar concentration ratio is 1:20.

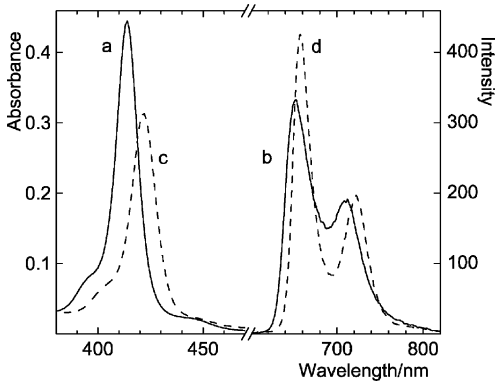

Fig. 2. Absorption and fluorescence emission spectra of 2.7 μM TMPTP (a, b) in comparison with the spectra of the 1:1 adduct TMPTP/d(A_8)d(T_8) (c, d). 20 mM phosphate buffer, pH 7.0, 100 mM NaCl, 47 μM d(A_8)d(T_8). Fluorescence spectra (b, d) were recorded using optically matched solutions at the excitation wavelength of 518 nm.

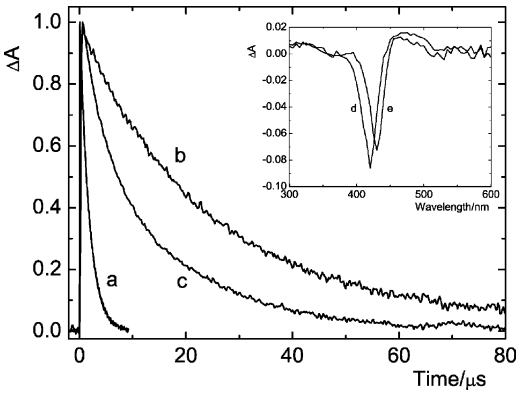

Fig. 3. Normalized quenching traces of the triplet states of TMPyP by oxygen. Free TMPyP recorded at 470 nm (a); intercalated TMPyP to [poly(dG-dC)]$_2$ recorded at 444 nm (b); and externally bound TMPyP to [poly(dA-dT)]$_2$ recorded at 470 nm (c). Inset: Difference absorption spectra of the triplet states of free TMPyP (d) and of TMPyP externally bound to [poly(dA-dT)]$_2$ (e). Air-saturated 20 mM phosphate buffer, 100 mM NaCl, pH 6.9, porphyrin/DNA (in base pairs) molar concentration ratio is 1:20, $\lambda_{exc} = 413$ nm.

bound porphyrin to other molecules in the environment. As a result, externally bound porphyrins exhibit only small red shifts of the Soret maximum (≤8 nm) and a small hypochromicity (≤10%) [79] (Fig. 1b, Fig. 2c). The same hypochromicity/sequence relation was observed for the triplet–triplet absorption spectra of TMPyP [87]. However, the absorption band is broadened up to 500 nm and is not shifted (Fig. 3d and e) [82,87,89].

2.1.1.1. Fluorescence. The correlation between binding modes of cationic porphyrins and their fluorescence properties has been investigated in detail [83,85–87,91,92]. The fluorescence emission band of TMPyP in aqueous solutions is broad (Section 2.3., Fig. 8a) with a low resolution of the Q(0,0) and Q(0,1) transitions. The featureless emission spectrum and a considerably low fluorescence lifetime of 5 ns (cf. with a typical value of 10–12 ns for metal-free porphyrins) is due to coupling the first excited state S_1 with a nearby charge transfer state CT_{in} (Table 2). Coupling in which an electron is transferred from the porphyrin core to an electron-accepting pyridinium group is facilitated in high polarity solvents and by a high degree of rotational freedom of these groups [93]. Upon binding of TMPyP to nucleic acids the original featureless emission spectrum is transformed into two distinct bands [83,86,91,92]. This splitting of the bands indicates that the electronic S_1–CT_{in} mixing within the bound excited molecule is less effective owing to a low polarity environment and confinement of TMPyP within binding sites thus hindering free rotation of the *N*-methylpyridinium groups. The change does not depend on the DNA sequence. Such fluorescence emission spectra are also typical for the TMPyP–cyclodextrin complex [94] (Section 2.3., Fig. 8b), TMPyP in methanol and other monomeric porphyrins [93]

in which internal electron transfer does not occur or is suppressed.

In contrast to the features of the emission spectra, the fluorescence quantum yields Φ_f of TMPyP vary significantly with the base content, i.e. with the binding mode. Upon external binding to [poly(dA-dT)]$_2$ the quantum yield Φ_f is greatly enhanced. It can be ascribed to changes of the local environment and limitation of the porphyrin accessibility to water molecules due to the matrix effect. The time-resolved fluorescence measurement provides additional information that the porphyrin environment is rather uniform even though the molecules are randomly distributed on the duplex exterior. This interpretation follows from the analysis of the fluorescence decay that is well fitted by a single lifetime of 12 ns, which is typical for porphyrin monomers [82,93]. In contrast, intercalation of TMPyP into [poly(dG-dC)]$_2$ causes a marked decrease of Φ_f and the fluorescence decay curves are best described with a bi-exponential fit $I(t) = A_1 \exp(-t/\tau_{f1}) + A_2 \exp(-t/\tau_{f2})$. The short-lived component has a lifetime of about 2 ns. This result suggests that due to intercalative binding at GC-rich regions fluorescence quenching is accompanied by the appearance of the short-lived fluorescence component. As the described effects of porphyrin interactions are cumulative, the influence of individual bases cannot be directly specified. For this reason it has been demonstrated that TMPyP forms 1:1 complexes with single nucleotides dAMP, dTMP and dCMP. This complexes have split fluorescence emission bands, enhanced Φ_f when compared to that of free TMPyP and the fluorescence lifetimes are increased from 5.29 to 11.3, 10.3, and 7.8 ns, respectively [95]. Similar fluorescence characteristics were discussed above for externally bound TMPyP on [poly(dA-dT)]$_2$. However, fluorescence emission of the TMPyP-dGMP complex is remarkably low and is best characterized by the excited singlet state lifetimes of 0.69 ns (a Lorentzian distribution) and 3.0 ns (a discrete component). The quenching between guanine and the excited singlet state of TMPyP has been shown to be reductive with the forward electron transfer rate of the order of $10^9\,s^{-1}$. Similarly, the fluorescence changes associated with intercalation of TMPyP at GC regions have been shown to be due to thermodynamically favored electron transfer from guanine residues to the excited singlet state of TMPyP [85,86,91]. This efficient quenching process can also account for the low value of Φ_T (see below). As demonstrated by experiments with *calf thymus* DNA, the value of Φ_f is between Φ_f's of TMPyP bound with [poly(dA-dT)]$_2$ and [poly(dG-dC)]$_2$, and fluorescence profile has two lifetimes of 2.5 ns and 11.0 ns. These results can be explained by two different localizations of the TMPyP molecules within the DNA duplex; intercalated molecules with the lifetime of 2.5 ns and externally bound with 11.0 ns. Similarly, the short fluorescence lifetime of about 3 ns of TMPyP bound to [d(TACGTA)]$_2$ or [d(TAGCTA)]$_2$ is due to electron transfer between guanine residues and TMPyP intercalated between 5′CG3′ or 5′GC3′ sequences [86]. The longer living component (8.0 or 10.4 ns) is probably given by contribution from both intercalated and externally bound TMPyP molecules. External binding of TMPyP to synthetic DNA hairpins has similar effects as described above, i.e. longer fluorescence lifetime of 8.6 ns, more intensive and sharpened emission spectra [83]. Reductive quenching of intercalated TMPyP by adjacent guanine residues depends on the base content of hairpin stems and it is a less favorable process as indicated by the less affected excited singlet state lifetimes of 4.2 and 5.8 ns.

Porphyrin TMPTP is bound exclusively on the exterior of nucleic acids because bulky peripheral substituents prevent intercalation between base pairs [57]. The fluorescence spectra of TMPTP consist of two bands that are red-shifted upon binding to single- or double-stranded oligonucleotides including *calf thymus* DNA (Fig. 2). The resolution of the Q(0,0) and Q(0,1) bands becomes more apparent and shows similarity to those of the emission spectra in less polar solvents. The fluorescence yields are slightly decreased and do not show any dependence on the base content of single- or double-stranded oligonucleotides. When all three methyl groups of the phosphonium substituents were replaced by more lipophilic phenyls to form BPPTP and TPPTP, the majority of the porphyrin molecules was spread on [poly(dA-dT)]$_2$ and [poly(dG-dC)]$_2$ exterior as extended assemblies [82]. The fluorescence lifetime of the assemblies is not affected by the type of polynucleotide and is ∼4 and ∼2 ns for BPPTP and TPPTP, respectively. The fluorescence lifetime of bound monomers is about 15 and 12 ns for BPPTP and TPPTP, respectively, again not showing any sequence dependence.

Also the luminescence intensity of CuTMPyP occurring from the $^{2,4}\pi$–π^* states depends on the binding mode [80,96]. While in aqueous solutions no detectable emission of CuTMPyP is found, in the presence of DNA a broad emission band is observed, centered at about 770 nm. Externally bound CuTMPyP has very little luminescence emission because an axially coordinated solvent or a nearby molecule on the duplex exterior can cause strong luminescence quenching. In contrast, the relatively large quantum yields up to about 10^{-4} with the emission lifetime of 22 ns were found for intercalated CuTMPyP between GC base pairs. The reason is that the porphyrin axial position is protected from attack by external molecules.

2.1.1.2. Triplet states. The formation and decay of the porphyrin triplet states can be recorded within the broad triplet–triplet absorption band in deoxygenated solutions (Fig. 3d and e). The triplet states decay by first-order kinetics. The available experimental data summarized in Table 2 show that intercalative binding between GC pairs typical for TMPyP, PdTMPyP(3) and PdTMPyP(4) causes considerable extension of the triplet lifetimes. Compared to intercalated PdTMPyP(3) and PdTMPyP(4), the lifetime of ^{3}PdTMPyP(2) is affected minimally as this compound cannot intercalate due to its rigidity. The external binding of

TMPyP with [poly(dA-dT)]$_2$ causes extension of the triplet lifetimes, the two different reported lifetimes [82,85], however, do not allow a precise assessment of the influence of the sequence of bases. The discrepancy in the experimental data probably consists in difficulty to completely remove oxygen from solutions. The triplet lifetime prolongation is caused by combination of several factors including confinement of the excited molecule within the solvent shell and changes in the solvent solvent–solute interactions due to reduced exposure of the excited molecules to solvent molecules.

The changes of Φ_T when binding to nucleic acids can be correlated with the formation of the excited singlet states (i.e. with Φ_f) (Table 3). The values of 0.44 and 0.95 were attributed to intercalated TMPyP in GC regions and to TMPyP located in external AT binding sites, respectively [85]. In the presence of nucleic acids containing GC-rich regions TMPyP intercalates and Φ_T decreases owing to thermodynamically favored electron transfer from G to the excited singlet state of TMPyP (see above) [85,95]. The intermediate value of Φ_T recorded for *calf thymus* DNA is due to mixing of both available binding modes.

2.1.1.3. Formation of $^1O_2$. The triplet states of porphyrins are quenched by molecular oxygen (Eq. (1)) with a bimolecular rate constant k_q of the order of $10^9\,M^{-1}\,s^{-1}$. In air-saturated aqueous solutions the kinetics of quenching are first-order (mono-exponential) and the lifetime of the triplet state is about 2 μs (Fig. 3a). The binding of porphyrins to nucleic acids causes a marked decrease up to 30 times in k_q depending on the nature of interacting components, in other words it causes an increase of the triplet state lifetimes. The kinetics of oxygen quenching become at least bi-exponential, which indicates the partition of porphyrin molecules among several distinct regions with differing oxygen accessibility. In the simplest case, the rate constant of the faster process is coincident with the k_q value of quenching of free (unbound) porphyrin in a solution and the slower process is attributed to quenching of bound porphyrin. The decay trace is then biphasic and the rate constants do not change with porphyrin/base pair molar concentration ratios, but the contribution of the respective components varies according to the equilibrium molar ratio of free/bound porphyrin in the ground state.

The triplet states of intercalated TMPyP (Fig. 3b), PdTMPyP(3) and PdTMPyP(4) are quenched mono-exponentially and their lifetimes are much longer (up to ca. 60 μs in air-saturated solutions) than those of free and externally bound porphyrins due to protection of porphyrin molecules from oxygen by the nucleic acid duplex. Oxygen accessibility to intercalated TMPyP does not depend on 5′CG3′ and 5′GC3′ sequences, which follows from comparison of the effects exerted by hexamers [d(TACGTA)]$_2$ and [d(TAGCTA)]$_2$. The resulting rate constants k_q are $1.3 \times 10^8\,M^{-1}\,s^{-1}$, which correspond with the lifetimes of about 30 μs in air-saturated solutions. Since the lifetime of TMPyP externally bound on hexamers is only about 7 μs, the TMPyP molecules are apparently more accessible to oxygen, but still the lifetime is much higher than 2 μs found for free TMPyP. Similarly, externally bound porphyrins PdTMPyP(2) and TMPTP have triplet lifetimes of 8–14 μs, i.e. more than four times higher than the free ones.

In all cases discussed above oxygen quenching of the triplet states is mono-exponential provided that only one binding mode is involved and concentration of free porphyrin is negligible. But, external binding of TMPyP to [poly(dA-dT)]$_2$ leads to bi-exponential kinetics with lifetimes of about 5 and 20 μs (Fig. 3c). This result is not consistent with fluorescence characteristics discussed above from which it follows that the porphyrin environment should be rather uniform. Kruk *et al.* have suggested that the appearance of two lifetimes is due to two populations of externally bound TMPyP differing in oxygen accessibility: TMPyP located in the major groove (face-on binding mode) is more accessible to oxygen than in the minor groove (edge-on binding mode) of the duplex [87]. With respect to binding of TMPyP to *calf thymus* DNA, two separate lifetimes 4.5 μs and 18.0 μs similar to those of ^{3}TMPyP on [poly(dA-dT)]$_2$ were reported while the lifetime of intercalated ^{3}TMPyP was not recognized because of its low contribution [87]. We have reinvestigated oxygen quenching of ^{3}TMPyP/*calf thymus* DNA by laser flash photolysis and found that the contribution of the respective components depended on a recording wavelength [89]. The recovery of the ground state recorded at the absorption maximum of intercalated TMPyP (445 nm) is dominated by a lifetime of 25.7 μs, i.e. the lifetime of intercalated TMPyP. We infer that the detailed kinetic analysis of oxygen quenching of ^{3}TMPyP can be used for recognition of respective binding modes. Biphasic kinetics attributed to two binding sites on the duplex exterior was observed only for TMPyP while the triplet states of PdTMPyP(2) and TMPTP indicate a uniform environment.

As pointed out earlier, $^1O_2$ is formed by quenching of the triplet states of both free and bound porphyrin monomers by dissolved oxygen regardless of the binding mode (Eq. (1), Scheme 1). The lifetime of $^1O_2$ in D_2O solutions is in the range 55–65 μs and the quenching rate constant of $^1O_2$ by nucleic acids themselves is low. Because the rise of the local concentration of $^1O_2$ is governed by the rate of triplet state quenching by oxygen and because collisional quenching of the triplet states of bound porphyrins is much slower than that of the free one, a much slower rate of the formation of $^1O_2$ can be expected. From this it follows that the rate of the $^1O_2$ formation produced by excited bound porphyrins and the rate of the decay of $^1O_2$ become comparable [57,87,88]. However, it does not necessarily mean that the total amount of $^1O_2$ produced is affected. For example, PdTMPyP(2), PdTMPyP(3) and PdTMPyP(4) in air-saturated D_2O exhibit comparable $\Phi_\Delta \approx 0.80$ regardless of the absence or presence of nucleic acids (Table 3) [88].

The Φ_T and Φ_Δ values of free TMPyP are equal and indicate that the triplet states are quenched by oxygen with 100% efficiency [87] (Table 3). This efficiency remains un-

changed for intercalated TMPyP in [poly(dG-dC)]$_2$ because both Φ_T and Φ_Δ are 0.44 and 0.47, respectively, giving S_Δ for this binding mode of 1.0 (Eqs. (6) and (7)). For binding TMPyP on [poly(dA-dT)]$_2$ and *calf thymus* DNA, the substantial differences between Φ_T and Φ_Δ give overall oxygen quenching efficiency of the triplet states S_Δ of 0.75 and 0.74, respectively.

In conclusion, to analyze the effect of nucleic acids on Φ_Δ of porphyrin sensitizers several opposite effects must be considered: (i) the increase of the lifetime of the triplet states upon binding; (ii) competitive processes which considerably decrease the quantum yields Φ_T and consequently Φ_Δ; (iii) molecular form of the bound porphyrin since fast non-radiative transitions occur within bound assemblies; (iv) structural control of porphyrin sensitizers concerning the mode of binding to nucleic acids. In some reported cases the most important feature characterizing the efficiency of $^1O_2$ production, i.e. Φ_Δ, remains unchanged even though the kinetics of $^1O_2$ formation slow down considerably. However, additional competitive processes can reduce the production of $^1O_2$ as observed for intercalated TMPyP. It is evident that the photophysical characteristics of porphyrin molecules as well as intermolecular interactions of the excited states with oxygen or other possible quenchers can produce new information on the microenvironment in which the porphyrin molecules are located.

2.1.2. Proteins

The non-covalent interactions between sensitizers, namely porphyrins or phthalocyanines, and proteins are essential for understanding the mechanism and efficiency of photoreactions on molecular and cellular level. The serum proteins, i.e. albumin, high-density lipoproteins and low-density lipoproteins [99], and antibodies can be used as natural carriers of the sensitizers, participating in transport to the tumor sites and in uptake into the cells. For these reasons most of the effort was devoted to characterize the binding process of synthetic porphyrins and phthalocyanines to serum proteins [11,53,64,65,100–112].

Proteins have single or multiple binding sites for porphyrins and phthalocyanines, including independent cooperative modes [101–106]. Binding influences distribution, metabolism and the molecular form of the sensitizers, e.g. their protonation, aggregation/dis-aggregation behavior and the concentration of the free molecules. Binding can alter their photophysical and photochemical properties. Hence, it is important to investigate how and to which extent it influences the photosensitized reactions. Conversely, porphyrins upon binding can induce structural modifications in the proteins [100–102]. In this section we will analyze typical changes of photophysical characteristics of the sensitizers when bound to proteins. The protein will be considered an inert matrix directing the photophysics of the bound molecules.

The electronic absorption spectra of porphyrins bound to proteins exhibit significant changes when compared with the corresponding monomer in an aqueous solution. The spectroscopic effects are due to changes in solvent–solute interactions as the polarity of the protein environment is lower than that of water. Binding is indicated by a red shift of the Soret band usually concomitant with some hypochromicity. A representative example is presented in Fig. 4a and b, showing that the Soret band of TPPS is shifted by 8 nm [53]. The visible Q bands are also shifted to longer wavelengths, e.g., from 633 to 646 nm. These binding-induced spectroscopic changes are often used for quantifying the affinity of the monomeric sensitizer to the respective binding sites of proteins characterized by a binding constant. Fluorescence properties are likewise very sensitive to the sensitizer environment and are particularly suitable for studying the binding event. The steady-state fluorescence spectra are red-shifted and two distinct peaks Q(0,0) and Q(0,1) are sharpened (Fig. 5). In addition, the overlap between the emission spectrum of the protein aromatic amino acid residues and the absorption spectrum of protein-bound

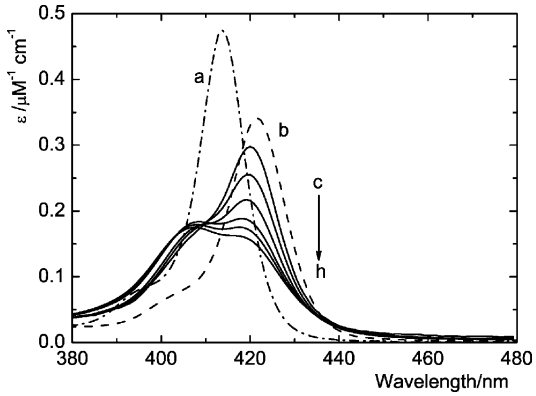

Fig. 4. Absorption spectra of 1.8 μM TPPS (a) and TPPS bound to BSA (b) in 7 mM phosphate buffer, pH 7.20, porphyrin/BSA = 0.16. Absorption spectra of TPPS in the presence of histone (solid lines); porphyrin/histone = 0.16, 0.32, 0.64, 0.78, 1.27 and 1.90 (c–h) in 7 mM phosphate buffer pH 5.70.

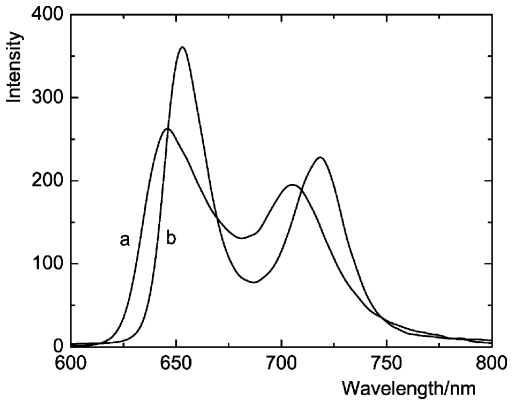

Fig. 5. Fluorescence spectra of TPPS (1 μM) in the absence (a) and presence of 10^{-4} M BSA (b). The samples had the same absorbance at the excitation wavelength of 516 (a) and 519 nm (b). 20 mM phosphate buffer, pH 7.0.

porphyrins favors fluorescence energy transfer to bound porphyrin [104–106,112]. Estimation of the energy transfer efficiency from proteins to bound porphyrins allows a detailed characterization of the protein binding sites.

2.1.2.1. Molecular form. Many porphyrins and phthalocyanines have a tendency to aggregate in aqueous solutions especially of high ionic strength. The addition of an excess of protein into such solutions usually breaks aggregates to monomers followed by the binding of the monomer [64,65,104,107,108]. The binding of monomers can be verified by UV-Vis and fluorescence spectroscopies because the spectroscopic features do not depend on the form of the sensitizer in solution. At porphyrin/protein molar ratios >1, TPPS aggregates whereas cationic TMPyP does not aggregate at all [107,108]. As a special case, we have previously reported aggregation of two sensitizers, TPPS and AlPcS, induced by binding to strongly basic nucleoprotein histone at low sensitizer/histone ratios of about 0.1 [53]. When bound to albumins at the same ratios no aggregation occurs. The typical spectroscopic features of TPPS aggregated on histone are broadening of the Soret band, a new band at about 405 nm and considerable hypochromicity (Fig. 4c–h). Evidently, shielding the negative sulfonate groups on the porphyrin periphery by the positive histone charges promotes aggregation through π–π interactions of the porphyrin units. Consequently, the fluorescence quantum yield of histone-bound TPPS (and similarly Φ_T and Φ_Δ as will be discussed below) decreases from the solution value of 0.060–0.035. Decrease of fluorescence is due to competitive radiationless processes (i.e. increase of efficiency of internal conversion) within bound aggregates, while an enhancement of intersystem crossing can be excluded since, in fact, Φ_T decreases.

Binding to the protein matrix also influences the acido-basic equilibrium of the sensitizer and hence aggregation of protonated porphyrin forms [53,105]. At lower pHs, two pyrrole nitrogen atoms of *meso*-tetraphenyl porphyrins having pK_a of 4.8 (e.g., TPPS) are protonated to the corresponding dianion (H_2^{2+}TPPS). When protein is added to H_2^{2+}TPPS, only TPPS is bound to protein indicating that the dianion is fully deprotonated before binding occurs. Evidently, electrostatic forces prevent the binding of porphyrin zwitterions with the cationic center and negatively charged periphery. The binding to the protein matrix also affects protonation of the porphyrin pyrrole nitrogen atoms in the triplet state [32,112]. Protonation of ^{3}TPPP or ^{3}TPPS to $^3H_2^{2+}$TPPP or $^3H_2^{2+}$TPPS is indicated by the appearance of a new intermediate at 500–510 nm in transient absorption spectra observed by means of laser flash photolysis. In contrast, protonation of the triplet states is completely suppressed in the presence of BSA. The bound excited molecules are separated from the bulk and the diffusion of H^+ from the bulk and/or from protonated amino acids in close proximity is hindered. Inhibition of protonation of the ground and triplet states of bound porphyrins confirms that porphyrins are placed in an environment with low content of water molecules.

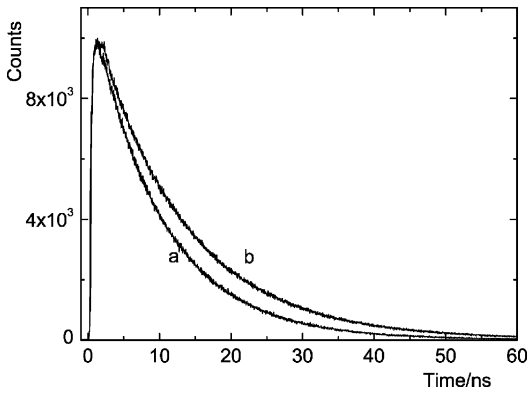

Fig. 6. Time-resolved fluorescence emission of TPPS (a) and TPPS bound to BSA (b); molar concentration ratio TPPS/BSA = 0.01, 20 mM phosphate buffer, pH 7.0, λ_{exc} = 390 nm, λ_{obs} = 650 nm. Decay curves are well described by a single exponential giving the lifetime of 9.6 (a) and 12.6 ns (b).

2.1.2.2. Fluorescence. Binding of porphyrins and phthalocyanines to proteins increases the lifetime of the excited singlet states [11,105,106,109,110,112,113]. The decay of fluorescence is characterized by a single long-lived fluorescence component (Fig. 6) [105,112] or displays complex kinetics that can be fitted by two or three exponential functions [11,106,109,110]. This could indicate that the respective fluorophores are located in different compartments within the protein matrix; in other words, it suggests the existence of several populations of the bound sensitizers. The analysis of decay kinetics yields fluorescence lifetimes and contributions of individual populations to the overall kinetics (Table 4). The two populations of lipoprotein-bound HP were correlated with the binding capacity of lipoproteins and with the efficiency of fluorescence energy transfer from the tryptophan residues of the protein to the porphyrin moiety [106]. Several populations were also reported for sulfonated aluminium phthalocyanines $AlPcS_n$ (n = 1, 2, 3,4) on HSA [11,109,110]. The fluorescence quantum yields Φ_f of $AlPcS_2$ and $AlPcS_3$ are 0.40 irrespective whether bound to HSA or free in water, while Φ_f of bound $AlPcS_1$ is considerably reduced. The analysis of the fluorescence decay led to the identification of three limiting environments: (i) excited $AlPcS_n$ molecules are in free contact with water (τ = 5.0 ns); (ii) water molecules are excluded or preferentially solvate the constituents of protein (τ = 6.7 ns); (iii) locations where additional quenching or interfacial effects occur (τ = 0.4–1.2 ns). Contributions of the respective components depend on the number of sulfonate groups and can be correlated with the hydrophilicity of the molecules increasing from $AlPcS_1$ to $AlPcS_4$. Consequently, the most hydrophobic $AlPcS_1$ partitions between the aqueous and protein phases (predominates i and iii), less hydrophobic $AlPcS_2$ and $AlPcS_3$ are bound at the protein surface and

Table 4
The photophysical characteristics of porphyrins bound to proteins in aqueous solution

Sensitizer	Φ_f	τ_f (ns)	τ_T (μs)	τ (μs)	$k_q \times 10^{-9}$ ($M^{-1}\,s^{-1}$)
ZnTDCSPP[a]	–	0.220	1650	7.4	0.48
ZnTDCSPP/HSA[a]	–	0.220	3300	19.4, 71	0.18, 0.05
HP/VLDL[b]	–	5.6, 17.9	31, 204	3.2, 8.5	1.0, 0.4
HP/LDL	–	2.1[b], 12.5[b]	68[b], 435[b], 200[i]	2.8[b], 5.3[b], 1.2[i]	1.2[b], 0.5[b]
PP/LDL[i]	–	–	200	2	1.8
TPPS	0.10[c], 0.06[h] 0.096[j]	9.8[c], 9.6[d], 8.3[j]	510[g], 410[j], 320[k]	2.0[g], 2.0[k], 2.3[k]	1.8[g], 1.6[j], 1.9[k], 1.7[k]
TPPS/HSA	0.10[c], 0.06[j]	12.9[c]	–	3.0[j], 24.0[j]	1.40[j], 0.17[j]
TPPS/BSA	–	12.6[d]	2400[g], 3200[k]	7.6[g], 18.0[k], 23.0[k], 66.0[k]	0.47[g], 0.21[k], 0.31[k], 0.055[k], 0.009[k]
TPPS/histone[g]	0.035	–	1000	9.2	0.39
TPPS/βLG[c]	0.11	12.8	–	–	–
TPPP[d]	0.064	9.1	300	2.4	1.5
TPPP/BSA[d]	0.052	12.1	–	13.8	0.26
SnTPPS[j]	0.001	–	420	1.9	1.9
SnTPPS/HSA[j]	–	–	–	6.4	0.65
TMPyP	0.044[l]	4.6[l], 5.29[m]	85[k], 23[k] 150[n], 170[l]	2.0[k], 2.0[o], 1.9[n]	1.9[k], 1.8[k], 1.86[o], 1.9[n]
TMPyP/BSA[k]	–	–	240, 110	3.4, 5.2, 330	1.1, 0.7, 0.093
$AlPcS_1$[e]	0.31	4.9	390	–	–
$AlPcS_1$/HSA[e]	0.25	1.1, 4.7, 7.4	760	–	–
$AlPcS_2$[e]	0.40	5.0	500	–	–
$AlPcS_2$/HSA[e]	0.40	1.2, 5.0, 6.4	1100	–	–
$AlPcS_2$/LDL[e]	–	–	1000	–	–
$AlPcS_3$	0.40[e], 0.47[j]	5.0[e], 5.5[j]	520[e], 270[j]	1.7[j]	2.1[j]
$AlPcS_3$/HAS	0.40[e]	0.3[e], 5.0[e], 6.4[e]	850[e]	2.4[j]	1.7[j]
$AlPcS_4$[e]	–	5.0	560	–	–
$AlPcS_4$/HSA[e]	–	5.0, 6.8	750	–	–
AlPcS[f]	–	–	440	2.1	1.7
AlPcS/BSA[f]	–	–	1160	18.8	0.19
ZnPcS[f]	–	–	165	1.9	1.9
ZnPcS/BSA[f]	–	–	300	16.2	0.22
$ZnPcS_3$[j]	0.35	2.8	205	1.6	2.2
$ZnPcS_3$/HSA[j]	0.35	–	–	3.0, 18.0	1.40, 0.23
PcS/BSA[f]	–	–	–	35.7	0.10

Symbols as in Table 2.
[a] [103], H_2O, pH 7.0.
[b] [106], phosphate buffer, pH 7.4.
[c] [105], H_2O, pH 7.
[d] [112], phosphate buffer, pH 7.0.
[e] [11,109,110], phosphate buffered saline, pH 7.4.
[f] [65], phosphate buffer, pH 7.1.
[g] [32,53], phosphate buffer, pH 7.2, τ_T of TPPS was measured at pH 10.0.
[h] [120].
[i] [111], phosphate buffered saline, pH 7.
[j] [64], neutral D_2O, τ of bound sensitizers in H_2O.
[k] [108], depending on pH: pH 4.0, 5.0 and 8.5.
[l] [85], phosphate buffer, pH 6.8.
[m] [95], phosphate buffer, pH 7.1.
[n] [82], phosphate buffer, pH 7.0.
[o] [87], D_2O phosphate buffer, pD 7.0.

within hydrophobic sites protected from water (predominates i and ii), and hydrophilic $AlPcS_4$ is attached to the protein surface (process i). Regarding bound $AlPcS_1$, the dominant contribution of the shortest lifetime process and the smallest Φ_f suggest that an additional quenching process is due to exciton interaction between closely spaced bound phthalocyanine units.

A very short intrinsic lifetime of the sensitizer monomer does not provide any additional information on the character of the binding sites. For example, the fluorescence lifetime of 220 ± 30 ps of ZnTDCSPP is unaffected by binding [103].

2.1.2.3. Triplet states. The triplet–triplet absorption bands of protein-bound porphyrins are broad and resemble those of free porphyrins [53]. But the lifetimes of the triplet states, recorded in the absence of oxygen, are much longer than the corresponding lifetimes of the free molecules in solution [11,53,65,106,109,110]. The reason is that the sensitizers are bound within the environment in which the rate of

solvent-enhanced deactivation of the triplet state is significantly lower than the rate in an aqueous solution. For example, the triplet state lifetimes of TPPS and AlPcS bound to BSA increase from 510 and 440 to 2400 μs [32,53] and 1160 μs [65], respectively (Table 4). The protein-bound sensitizers possess a single triplet lifetime with the exception of HP [106], where two lifetime components are explained by location of HP in two different environments within the lipoprotein matrix. The lifetimes up to several milliseconds may enable additional photochemical processes with components of the protein matrix.

The kinetics of quenching the triplet states by dissolved oxygen (Eq. (1)) can also be multi-phasic and best fitted by several exponential terms. The multi-phasic kinetics can be attributed to a combination of three effects: the equilibrium between free/bound porphyrin, several populations of protein-bound porphyrin molecules differing in oxygen accessibility and dynamic changes in equilibrium conformations of protein causing distinct positions of the sensitizer with regard to the aqueous phase. The fraction of free sensitizer depends on the concentration of protein and can be minimized by high molar excess of protein. Generally, there is at least one population of the triplet states, well shielded from oxygen, that is quenched by oxygen with a rate constant of about one order of magnitude lower ($k_q \sim 10^8\ M^{-1}\ s^{-1}$) than that of free porphyrin ($k_q \sim 10^9\ M^{-1}\ s^{-1}$) (Table 4). For instance, one population of ^{3}ZnTDCSPP and ^{3}TPPS is buried deep in the protein matrix with an even lower oxygen accessibility because the triplet states are quenched with k_q of 5.0×10^7 and $9\times10^6\ M^{-1}\ s^{-1}$, respectively [103,108]. On the other hand, if the sensitizer is located close to the interface with a solvent and readily accessible to oxygen, the rate k_q remains nearly unchanged with the value of the order of $10^9\ M^{-1}\ s^{-1}$ [64,106]. However, there is some uncertainty at this point because it can be difficult to differentiate between interface bound and free sensitizers. It has been reported that binding $AlPcS_3$ has little effect on k_q since the values of bound and free $AlPcS_3$ are 1.7×10^9 and $2.1\times10^9\ M^{-1}\ s^{-1}$, respectively [64]. On the other hand, the corresponding rate constant of AlPcS (sulfonation degree 2.2) was reported to decrease about ten times to $1.9\times10^8\ M^{-1}\ s^{-1}$ [65]. In this study the kinetics of oxygen quenching were analyzed using a model, in which the "slow" process was attributed to bound AlPcS and the "fast" process to free AlPcS, allowing the calculation of respective equilibrium molar fractions for a given molar ratio of both components. Because for the analogous pair $ZnPcS_3$ and ZnPcS (sulfonation degree 2.5) were reported almost identical values for the bound forms, namely 2.3×10^8 [64] and $2.2\times10^8\ M^{-1}\ s^{-1}$ [65], the discrepancy between quenching of $AlPcS_3$ and AlPcS cannot be due to the differences in the sulfonation degree. More probably, D_2O used in [64] shifts the equilibrium towards free $AlPcS_3$ or the exchange between free and bound $AlPcS_3$ is faster and occurs within the lifetime of the triplet states.

The photophysical characteristics summarized in Tables 4 and 5 document that binding of the sensitizers does not inhibit excitation to the triplet states, although the binding does affect the rate constant k_q and hence the triplet lifetimes in the presence of oxygen. As a result, the longer lifetime (cf. 2.1 and 18.8 μs for free and bound AlPcS in air-saturated phosphate buffer [65]) implies a relatively slow growing-in of the $^1O_2$ concentration according to Eq. (1). The reported values of Φ_T do not change upon binding indicating that the bound sensitizers retain their $^1O_2$ producing capacity (Table 5). In the case of $AlPcS_1$ the value of Φ_T decreases in accord with the prevailing short-lived fluorescence component, signalizing another quenching mechanism different from that producing $^1O_2$ [11,109]. The considerable decrease of Φ_T from 0.76 to ≤0.2 for histone-bound TPPS is apparently caused by binding-induced aggregation of TPPS [53].

Table 5
Quantum yields of the triplet states (Φ_T) and of the singlet oxygen formation (Φ_Δ) of protein-bound porphyrins

Sensitizer	Φ_T	Φ_Δ
ZnTDCSPP[a]	0.96	0.74
ZnTDCSPP/HSA[a]	–	0.76
TPPS	0.76[b], 0.79[f]	0.57[d], 0.64[f]
TPPS/histone[c]	≤0.2	<0.1
TPPS/HSA[f]	0.66	0.66
SnTPPS[f]	1.0	0.77
SnTPPS/HSA[f]	1.0	0.81
$AlPcS_1$[e]	0.21	–
$AlPcS_1$/HSA[e]	0.10	–
$AlPcS_2$[e]	0.17	–
$AlPcS_2$/HSA[e]	0.18	–
$AlPcS_3$	0.17[e], 0.46[f]	0. 34[f]
$AlPcS_3$/HAS	0.18[e], 0.43[f]	0.32[f]
$ZnPcS_3$[f]	0.51	0.36
$ZnPcS_3$/HSA[f]	0.62	0.51

[a] [103], H_2O, pH 7.0.
[b] [121], phosphate buffer, pH 7.4.
[c] [53], phosphate buffer, pH 7.2.
[d] [122], average literature value.
[e] [11,109,110], phosphate buffered saline, pH 7.4.
[f] [64], neutral D_2O.

Not many results on $^1O_2$ formation sensitized by protein-bound porphyrins or phthalocyanines have been published so far. From the values of Φ_Δ listed in Table 5, it is apparent that the non-covalently bound sensitizers remain good producers of $^1O_2$. In this context very little attention has been devoted to the photophysics of sensitizers non-covalently interacting with protein constituents—amino acids residues. The stacking interactions between the aromatic side-chains of amino acids and water-soluble metalloporphyrins [114,115] or porphyrins [32,115] have been reported previously. Hence, additional highly competitive processes as photoinduced electron transfer from the tyrosine or tryptophan moiety to several porphyrins excited to the triplet states [116,117] can affect the overall photophysics of the sensitizers. As far as we know the organization and distribution of the excited sensitizer within the protein matrix can affect the efficiency of the sensitizing process due to sensitizer aggregation or to

its localization in proximity to readily oxidizable amino acid residues (e.g. Trp, His, Met, Cys) consuming $^1O_2$. Thus, HSA itself removes $^1O_2$ from the sensitizing system with the bimolecular rate constant of $(5 \pm 3) \times 10^8\ M^{-1}\ s^{-1}$ [64].

The available data show that the sole binding of the sensitizer does not affect the generation of $^1O_2$ provided that the sensitizer does not aggregate or is not bound close to protein constituents that quench the excited states (electron/energy transfer processes) [53,64,103] (Table 5). Furthermore, non-covalent labeling of proteins with porphyrins or phthalocyanines can provide a tool for selective denaturation [118] and for probing the topology of the binding sites, conformation changes, subunit interactions, characteristics of binding, and exposure of local sites to solvent molecules. The binding-induced spectroscopic changes could even indicate the presence of different proteins [119].

2.2. Liposomes

The photophysical properties of porphyrinoid sensitizers in microheterogeneous systems, such as liposomes, micelles, emulsions and colloids are of current interest [5,6,123,124]. The photophysical properties and production of $^1O_2$ are sensitive to the interfacial characteristics of specific microdomains that host the sensitizer. The assessment of these photophysical and photochemical parameters can be used to probe the surroundings of the sensitizer and its localization. Liposomes are often used as simple models for mimicking cellular membranes and as carriers for transport of hydrophobic sensitizers to cells.

Liposomes are microscopic spherical or ellipsoidal vesicles, single or multi-compartmental, that are formed when amphiphilic lipids containing two hydrocarbon chains and a polar group (e.g. phospholipids) are hydrated. When mixed with water the amphiphilic lipids are aligned side by side to form a bilayer membrane, which inside a vesicle encloses a pool of water (Scheme 6). The properties of vesicles are determined by their composition, the number of compartments (uni- or multilamellar, uni- or multivesicular), size (small $\leq$100 nm, large 100–500 nm, and giant >1 μm in diameter) and phase transition temperature (below this temperature a bilayer is more regular and loses its fluidity) [125]. Liposomes most frequently studied are phospholipids DPPC, DMPC, DOPC, POPC, DOPS and EPC.

The binding of the sensitizers originates from a combination of hydrophobic and electronic interactions and the distribution in these environments is influenced by the hydrophobic/hydrophilic character of the surrounding medium and by the presence of electrostatically charged interfaces. The sensitizers can be incorporated into a lipid bilayer or encapsulated into a water pool (Scheme 6).

Three main effects of liposomes on the sensitizers were described: (i) *Monomerization effect*. Monomerization of aggregated hydrophobic sensitizers occurs as a result of localization of the sensitizer molecules within hydrophobic bilayers [126–128]. (ii) *Concentration effect*. The local concentration of the sensitizer inside a vesicle is larger, by several orders of magnitude, than in a solvent. High local concentrations can lead to structurally controlled aggregation process in liposome bilayers, i.e. the effect inverse to (i) [129]. (iii) *Viscosity effect*. After incorporation to a liposome bilayer, the sensitizer is located in a structured microenvironment. Increased microviscosity slows down internal movements of the embedded molecule and all collisional processes of excited states by restricting their diffusion motion [128].

The balance between the hydrophobicity/hydrophilicity of the sensitizer and lipid bilayers influences the distribution of the sensitizer over different regions of the liposomal structure. Hydrophobic sensitizers penetrate into a lipidic bilayer. Hydrophilic sensitizers are usually located on the surface of liposomes or in an endoliposomal aqueous compartment near the polar heads, weakly interacting with the hydrophobic region of liposome [126]. The hydrophobic parts of amphiphilic sensitizers are situated in a microenvironment of low polarity (a lipidic bilayer) while the charged peripheral substituents are oriented towards the polar heads of lipid molecules [130].

2.2.1. Absorption and fluorescence

After incorporation of the sensitizers into liposomes the corresponding absorption and fluorescence emission bands are usually red shifted, and fluorescence intensity and fluorescence anisotropy are increased [6,131–137]. These spectroscopic changes provide a tool for the investigation of the sensitizer uptake and distribution in liposomes. Typically, HP and DP exhibit a red shift of the absorption and emission maxima of about 10–20 nm after incorporation into the liposome matrix [134]. Such large red shifts in absorption spectra are often ascribed to monomerization of aggregated

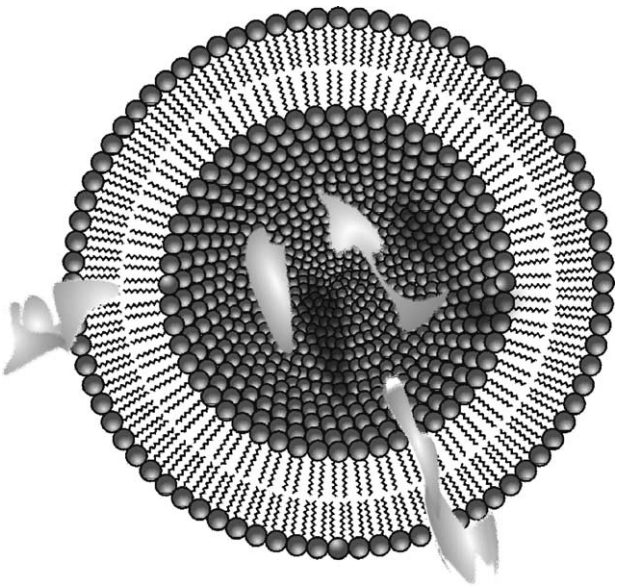

Scheme 6. Cross section of the unilamellar liposome with the incorporated (bilayer) and encapsulated (water pool) sensitizer molecule.

sensitizers. In contrast, polar UP is monomeric in aqueous media and shows only minor spectroscopic changes. This indicates that UP is predominantly confined in the endoliposomal aqueous compartment because its microenvironment is not changed after interaction with DPPC liposomes [131].

Incorporation of the porphyrin sensitizer into a lipid bilayer affects the conformational dynamics of the molecule in the ground (S_0) and excited singlet (S_1) states. These changes influence the Stokes shift, i.e. the energy difference between absorption and emission bands from lowest vibration levels of the S_0 and S_1 states. Ordered lipid bilayers have a strong influence on *meso*-tetraarylporphyrins because the decrease of the dihedral angle between the planes of the porphyrin unit and *meso*-phenyl occurring in the S_1 state allows greater conjugation of π orbitals [138]. Thus, TPPB exhibits a marked decrease of the Stokes shift after incorporation into DPPC liposomes, while with TTP the shift remains almost unchanged. The reason is that the bulky 3,5-di-*tert*-butylphenyl groups of TPPB restrict the rotation of the phenyls around the C–C linkage in bilayers.

Furthermore, the placement of the sensitizer in a liposome bilayer is indicated by fluorescence anisotropy [131]. The anisotropy values reveal the degree of a restriction of rotational freedom of the imbedded molecules in the anisotropic membrane environment [6,126,136]. The anisotropy is sensitive to the phase transition temperature of liposomes. Hence, the temperature dependent anisotropy can be used to probe the physical properties of various domains of vesicles.

2.2.2. Excited states

In a series of liposome-bound porphyrins going from tetracationic TMPyP to monocationic MPyP the values of Φ_f increase from 0.044 to 0.077 [126]. The order of increasing hydrophobicity TMPyP < TrMPyP < BMPyP < MPyP then follows. The most hydrophobic MPyP has the same Φ_f in liposomes and in non-polar $CHCl_3$, i.e. 0.077 and 0.075, respectively. The least hydrophobic TMPyP has the same Φ_f of 0.044 in water as in liposomes. The results suggest that the distribution in liposomes depends on porphyrin hydrophobicity: MPyP and BMPyP can penetrate into the lipidic phase while TMPyP is located near the polar heads of the lipidic molecules and feels the aqueous pool rather than the hydrophobic environment. Similarly, carboxylic porphyrins, HP and DP, show increased Φ_f when passing from an aqueous solution to liposomes [6,134,139]. The fluorescence enhancement was also reported for Photofrin II and HPD in the presence of liposomes attributed to increased surrounding microviscosity that weakens non-radiative processes such as physical quenching by solvent molecules [128,137]. Phthalocyanines *cis*-$AlPcS_2$ [140] and $MgPcB_4$ [141] behave similarly to MPyP having the same Φ_f in liposomes and $CHCl_3$. The decrease of Φ_f from 0.48 to 0.23 by increasing concentration of $AlPcS_2$ in DPPC is due to the concentration effect.

In the absence of oxygen the triplet state lifetime of *cis*-$AlPcS_2$ in the structured microenvironment provided by liposomes increases from 550 to 1200 μs because the higher microviscosity slows down collisional deactivation of the triplet states by restricting their diffusion [140]. The triplet states of HP also decay by first-order kinetics, however, a direct interaction between ^{3}HP and the phosphatidylcholine molecule of liposome occurs [142]. In DMPC liposomes the decay of ^{3}MPyP, unlike ^{3}TMPyP, is complex and can be analyzed with two discrete lifetimes of 24 and 133 μs in H_2O, and 16 and 102 μs in D_2O [126]. Similarly to the matrix effect of nucleic acids or proteins, such complex decay can be rationalized by different localizations of MPyP differing in imbedded depth in a bilayer. Because of a random distribution of the sensitizer molecules within a liposome bilayer, rather than two specific lifetimes a distribution of lifetimes would better characterize the overall process. The triplet states of TMPyP decay mono-exponentially with lifetimes of 108 μs in H_2O and 173 μs in D_2O. This substantial isotopic effect, not observed with MPyP, confirms localization of TMPyP in an environment accessible for solvent molecules.

In the presence of oxygen the triplet state deactivation is determined by oxygen quenching, which is controlled by diffusion of oxygen from the bulk to a vesicle membrane. In most cases the triplet states are quenched by first-order kinetics in air-equilibrated liposomal solutions [143]. The quenching rates significantly increase around the liposome phase transition temperature because the excited molecules experience an environment with a three to four times increased diffusion coefficient of O_2 [143].

The effect of liposomes on Φ_T depends on the sensitizer behavior in aqueous solutions. Both MPyP and TMPyP have Φ_T of about 0.7 in DMPC liposomes, similar to the value of TMPyP in homogeneous aqueous solutions [126]. Interestingly, in liposomes no isotopic effect of D_2O is observed. $AlPcS_2$ in H_2O, methanol and DPPC liposomes has Φ_T of 0.17, 0.24 and 0.24, respectively [140]. An increasing concentration of *cis*-$AlPcS_2$ in DPPC liposomes causes quenching of the triplet states due to the concentration effect (similar to Φ_f discussed above); Φ_T can be as low as 0.04. The increase of Φ_T when compared to an aqueous solution is usually connected with sensitizer monomerization. Hence BC exhibits a fourfold enhancement when going from a neutral phosphate buffer ($\Phi_T = 0.095$) to DMPC ($\Phi_T = 0.4$) [144]. As DMPC shifts the monomer–dimer equilibrium of BC to the monomer, the low Φ_T in a phosphate buffer is ascribed to the fact that the triplet states are formed only by the BC monomer. Although BC is monomeric in DMPC, nearly half Φ_T than in methanol indicates that microviscosity is an important factor.

2.2.3. Formation of $^1O_2$

The major factors affecting quantum yields of the excited states and consequently of Φ_Δ in organized liposomal media are as follows [128]: (i) *Viscosity*. Increased microviscosity causes an enhancement of the fluorescence intensity. (ii) *Intersystem crossing*. The non-radiative relaxation channels

are weakened by higher microviscosity. (iii) *Monomerization*. Dimers or higher aggregates produce little or no $^1O_2$. (iv) *Concentration*. The local concentration of the sensitizer is different from the concentration in solution. (v) *Competing reaction channels*. Oxidation of oleic acid side chains in EPC consuming $^1O_2$ is an example [145]. Therefore, it is recommended to use phospholipids with an aliphatic hydrocarbon chain (e.g. DPPC), which endows liposomes with photochemical inertness [131]. Some selected data on Φ_Δ are summarized in Table 6. The Φ_Δ values in liposomes are compared to those in water or organic solvent according to hydrophilicity/hydrophobicity of the sensitizer. However, because the production of $^1O_2$ by liposome-bound sensitizer is controlled by many factors, often acting against each other, the overall effect of liposomes (i–v) on Φ_Δ can hardly be generalized. An unusual increase of Φ_Δ in the presence of liposomes can be attributed to the monomerization effect of the vesicles. *Vice versa*, a decrease of Φ_Δ can be ascribed to aggregation occurring in liposomes due to the concentration effect.

The measurement of Φ_Δ itself can be problematic and the results can depend on the method used. Indirect chemical quenching methods in particular can produce misleading results due to: (i) Differing localization of the sensitizer and target molecules (target localized in other vesicles, target localized outside the vesicles, both inside the same vesi-

Table 6
Quantum yields of the singlet oxygen formation (Φ_Δ) of porphyrinoid sensitizers in liposomes

Sensitizer	Phase	*d* (nm)	Φ_Δ	Method	Reference
MpyP	Chloroform	–	0.78	TRIL	[126]
MpyP	D_2O/DMPC	100	0.64	TRIL	[126]
MpyP	D_2O/DPPC	50	0.38	TRIL	[126]
BMPyP	Chloroform	–	0.75	TRIL	[126]
BMPyP	D_2O/DMPC	100	0.57	TRIL	[126]
BMPyP	D_2O/DPPC	50	0.40	TRIL	[126]
TrMPyP	Chloroform	–	0.81	TRIL	[126]
TrMPyP	D_2O/DMPC	100	0.91	TRIL	[126]
TrMPyP	D_2O/DPPC	50	0.63	TRIL	[126]
TMPyP	D_2O	–	0.75	TRIL	[126]
TMPyP	D_2O/DMPC	100	0.85	TRIL	[126]
TMPyP	D_2O/DPPC	50	0.65	TRIL	[126]
HPD	PB (pH 7.4)	–	0.06	RNO	[127]
HPD	PB (pH 7.4)/EPC	–	0.87	RNO	[127]
UP	PB (pH 7.4)	–	0.71	RNO	[127]
UP	PB (pH 7.4)/EPC	–	0.92	RNO	[127]
HP	PB (pH 7.4)	–	0.47	RNO	[127]
HP	PB (pH 7.4)/EPC	–	0.77	RNO	[127]
PdTPP[a]	Toluene	–	0.86	TRIL	[148]
PdTPP	D_2O/DPPC	–	0.16	TRIL	[148]
PdTEPP	Toluene	–	0.86	TRIL	[148]
PdTEPP	D_2O/DPPC	–	0.09	TRIL	[148]
PO	D_2O/DPPC	52	0.17–0.37	TRIL	[146]
TPrPO	Benzene	–	0.37	TRIL	[149]
TPrPO	D_2O/DPPC	52	0.37	TRIL	[149]
TPrPO	D_2O/DPPC	52	0.22–0.37	TRIL	[146]
ZnPc	Benzene	–	0.50	TRIL	[150]
ZnPc	TRIS (pH 7.4)/DPPC	52	0.7	DPBF	[147]
ZnPc	D_2O/DPPC	52	0.47	TRIL	[146]
$ZnPc(OH)_4$	H_2O/EPC	–	0.005	DMA	[151]
BC	PB (pH 7.0)	–	0.05	TRIL	[144]
BC	Methanol	–	0.36	TRIL	[144]
BC	PB (pH 7.0)/DMPC	90	0.33	TRIL	[144]
MgTBP	Benzene	–	0.34	DMA	[152]
MgTBP	Methanol	–	0.126	DMA	[152]
MgTBP	H_2O/EPC	–	0.019	DMA	[151]
ZnTBP	Benzene	–	0.497	DMA	[152]
ZnTBP	H_2O/EPC	–	0.023	DMA	[151]
Photofrin II	D_2O	–	0.16	O_2 depletion	[153]
Photofrin II	H_2O/EPC	–	0.191	DMA	[151]
Photofrin II	PB/EPC	–	0.87	RNO	[127]

The diameter *d* of liposomes and the method of Φ_Δ determination are given where specified. Abbreviations: PB, phosphate buffer; TRIL, time-resolved infrared luminescence; RNO, bleaching method using *p*-nitroso-*N*,*N*′-dimethylaniline; DMA, fluorescence method using 9,10-dimethylanthracene; DPBF, bleaching method using diphenylisobenzofuran.

[a] All *meso*-substituted Pd porphyrins in [148] behave as presented PdTPP and PdTEPP.

cle but spatially separated, *etc*.) [5,128]. The rate constants of oxidation of a quencher with $^1O_2$ are much smaller in the presence of liposomes, especially when both the sensitizer and quencher are incorporated in liposomes. (ii) Size of liposomes because inter- and intravesicular distances can be comparable or larger than the average diffusion path of $^1O_2$ [5]. (iii) Consumption of $^1O_2$ by liposomes containing unsaturated fatty acids [145]. iv) Secondary reactions of a quencher in bilayers (cf. ZnPc with Φ_Δ of 0.47 and 0.7 determined using TRIL and quencher DPBF, respectively [146,147]).

In conclusion, liposome-bound sensitizers produce effectively $^1O_2$. After $^1O_2$ is produced it diffuses freely between the lipidic and aqueous phases. In the absence of any quenching process (low physical quenching, photochemical inertness of liposomes, no singlet oxygen quenchers) the equilibrium distribution of $^1O_2$ between the lipid bilayer and aqueous phases is attained before $^1O_2$ decays. Small unilamellar vesicles ensure that $^1O_2$ is mostly located in the aqueous phase. Although the lifetime is different in both phases, as the lipid volume represents only several percent of the total volume, the lifetimes of $^1O_2$ are practically independent of the localization and type (hydrophilic or hydrophobic) of the sensitizer and correspond to those in homogeneous aqueous solutions [126,146].

2.3. Container molecules

Container molecules represent a class of macrocyclic host compounds having internal cavities capable of encapsulation of small molecules [154–156]. They have openings of various sizes that allow guest molecules to enter and leave. It was also demonstrated that self-complementary host molecules could dimerize to form spherical capsules in which small molecules are locked. Porphyrinoid sensitizers are evidently too large to be completely encapsulated in the inner cavity. Instead, host–guest complexes can be formed incorporating a part of the sensitizer (e.g. phenyls of *meso*-substituted tetraphenylporphyrins) with the rest of the porphyrin molecule protruding to the bulk. Another binding mode is fixing the sensitizer at the host exterior.

The hosts of sensitizers should control the binding event, minimally affect the formation of $^1O_2$ and release guests under defined conditions. From the variety of container molecules only two macrocyclic hosts, cyclodextrins (CD) and calix[*n*]arenes have been investigated so far as potential carriers for porphyrin sensitizers. Here, we summarize the photophysical properties of the porphyrin sensitizers bound to CD and calix[*n*]arenes and compare the influence of both hosts.

2.3.1. Cyclodextrins

The most common cyclodextrins consist of 6, 7 or 8 α-1,4-D-glucopyranose units arranged to a truncated cone and denoted as αCD, βCD and γCD, respectively (Scheme 7) [157–159]. The interior, lined with C–H groups and glycosidic oxygen bridges, is hydrophobic in comparison with the exterior that is hydrophilic due to hydroxyl groups. Consequently, CDs are water-soluble, form inclusion host–guest complexes with a variety of guest molecules, and might influence their photophysical and photochemical properties. The substances are bound in the cavity by hydrophobic forces and hydrogen bonding. On account of the hydrophobic interior of CDs even hydrophobic substances can be transferred into aqueous solutions. The pharmaceutically useful CD derivatives can be classified as hydrophilic, hydrophobic and ionic depending on the functionalization of the hydroxyl groups. Cyclodextrins are frequently used in pharmacology to improve the resistance of pharmaceuticals to thermal and oxidative degradation, limit side effects, increase solubility, and prevent aggregation [159,160].

Surprisingly, only the photophysical properties of anionic *meso*-tetraphenylporphyrins and cationic TMPyP bound to CDs have been reported until now. It is evident that binding of porphyrins can be sensitive to the nature and size of their peripheral substituents, preferentially incorporated into the cavity. The equilibrium between the sensitizer (Sens) and CD proceeds in two steps:

$$\text{Sens} + \text{CD} \rightleftharpoons \text{Sens-CD} \quad (13)$$

$$\text{Sens-CD} + \text{CD} \rightleftharpoons \text{Sens-(CD)}_2 \quad (14)$$

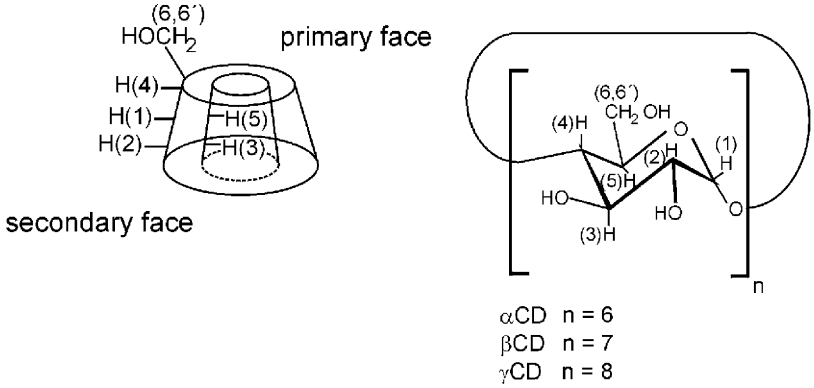

Scheme 7. Schematic representation of CDs.

The fraction of the 1:1 and 1:2 host–guest complexes is controlled by binding conditions. The binding constants depend strongly on the cavity size and functionalizing CDs and are in the range of 10^3–10^5 M^{-1} [161–163]. The binding modes of anionic *meso*-tetraphenyl substituted porphyrins can be classified into three types [161,163–165]:

(i) Inclusion through the secondary face. This is a typical mode for βCD and functionalized βCDs and has the strongest effect on binding, spectroscopic and photophysical quantities of monomeric porphyrins. For example, the 4-sulfonatophenyl or 4-carboxyphenyl substituents penetrate deeply into the cavity with the sulfonic or carboxylic groups oriented towards the primary hydroxyl groups.
(ii) Inclusion through the primary face. This mode is typical for γCDs. The size of the secondary face is larger than in βCDs and, therefore, the inclusion from the primary face is more favorable.
(iii) Non-specific external binding. The mode comprises direct contacts between the CDs exterior and porphyrin monomer or aggregate and is the least noteworthy for carrying sensitizers. Recent results suggest that cationic TMPyP interacts in this way [166].

Binding influences the molecular form of porphyrins similarly to the effects described in Sections 2.1 and 2.2. Aggregates are usually monomerized since the driving force to form complexes exceeds the energy gain from stacking the porphyrin units. The higher is the affinity of CDs expressed by the binding constant, the more pronounced is monomerization. Furthermore, the pyrrole nitrogen atoms of anionic *meso*-tetraphenylporphyrins are protonated at pHs below pK_a (about 4.8). Binding porphyrins to CDs prevents the protonation of these nitrogen atoms and induces dis-aggregation of J-aggregates [162]. Thus, the photophysical properties of CD-bound porphyrins can be ascribed to the bound monomeric species with part of the porphyrin molecule confined in the CD cavity and separated from a bulk solution.

Titration of a porphyrin solution with CDs leads to a red shift of the Soret band indicating the presence of Sens-CD and Sens-$(CD)_2$ complexes in the equilibrium. The shift reflects the electronic perturbations arising from solvent effects and from changes in the solvent–solute dipole interactions caused by reduced exposure of the solute to water. Binding is also indicated by a red shift of the fluorescence emission bands copying the shift of the absorption spectra (Fig. 7). The fluorescence quantum yields are only slightly affected (Table 7). But, binding of TPPS or TPPC within βCD-dimers decreases fluorescence intensities depending on the nature of connecting flexible link between βCDs [167]. Unexpectedly, a strong effect on fluorescence emission spectra is observed for cationic TMPyP in the presence of hpCDs [94]. The fluorescence emission band of free TMPyP is broad (Fig. 8a) with low resolution of the Q(0,0) and Q(0,1) bands (as discussed in Section 2.1.1.1). Interaction with hpCDs

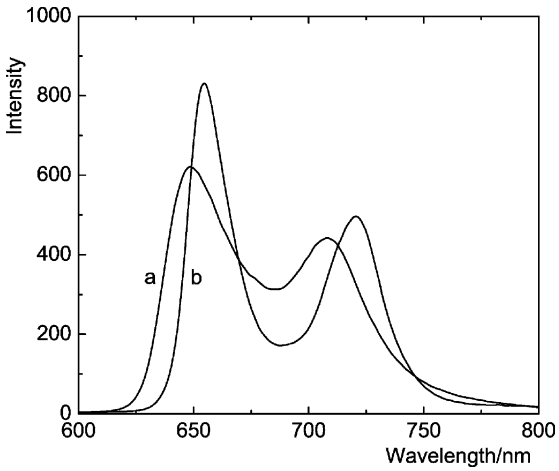

Fig. 7. Fluorescence spectra of TPPS (1 μM) in the absence (a) and in the presence of 10^{-4} M hpβCD (b). Optically matched samples at λ_{exc} = 416 nm in 20 mM phosphate buffer, pH 7.0.

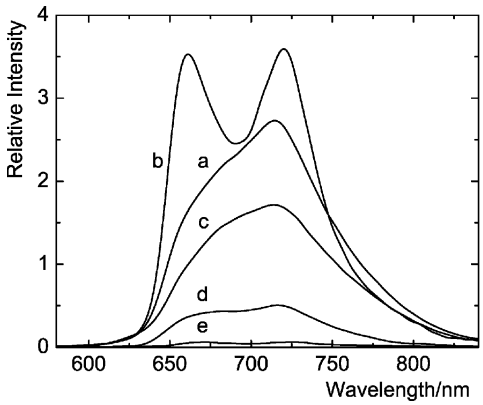

Fig. 8. Steady-state fluorescence spectra of TMPyP (a) and of its complexes with hpβCD (b), calix[4]arene-4-tetrasulfonate (c), calix[6]arene-4-hexasulfonate (d), and calix[8]arene-4-octasulfonate (e). All measurements were performed in 20 mM phosphate buffer, pH 7.0, using optically matched solutions at λ_{exc} about 520 nm.

is accompanied by an increase of the fluorescence quantum yield from 0.046 to 0.058 (Table 7) and by a dramatic change of fluorescence emission spectra (Fig. 8b). These changes were used to determine the complex stoichiometry (1:1) and binding constant (5.4×10^3 M^{-1}) (Fig. 9). The fluorescence spectrum of the TMPyP–hpβCD complex consists of two separate bands at 660 and 720 nm and resembles the spectra of monomeric porphyrins [93,168] indicating that intramolecular charge transfer within the porphyrin moiety responsible for the emission band broadening was eliminated. A similar effect is observed for native CDs [166].

The reported photophysical properties of the porphyrin–CD complexes are summarized in Table 7. Binding does not change Φ_T and the spectroscopic features of the triplet–triplet spectra. Still, the lifetime of the triplet states of the bound porphyrins in the absence of oxygen is considerably extended. This lifetime increase can be attributed to the combination of two factors: exclusion of water molecules

Table 7
The photophysical characteristics of porphyrins bound to CDs in aqueous solution

Complex	Φ_f	τ_T (μs)	τ (μs)	$k_q \times 10^{-9}$ ($M^{-1}s^{-1}$)	Φ_T	Φ_Δ
TPPS	0.06[d]	290[a]	2.0[a]	1.8[a]	0.76[e], 0.79[i]	0.62[f]
TPPS/hpαCD[a]	–	290	2.2	1.6	–	–
TPPS/hpβCD[a]	0.05	2000	11.9	0.30	0.76	0.60
TPPS/hpγCD[a]	–	2100	3.6	1.00	–	–
PdTPPS	0	200[b]	2.0[b]	1.80[b]	0.63[b], 0.63[g]	0.50[b], 0.49[g]
PdTPPS/αCD[b]	0	200	2.0	1.80	0.62	0.50
PdTPPS/hpαCD[b]	0	200	2.8	1.30	0.64	0.50
PdTPPS/βCD[b]	0	220	3.7	0.96	0.78	0.50
PdTPPS/hpβCD[b]	0	490	10.2	0.35	0.79	0.60
PdTPPS/γCD[b]	0	230	3.9	0.91	0.74	0.50
PdTPPS/hpγCD[b]	0	230	6.0	0.60	0.73	0.50
ZnTPPS	0.04[b]	1100[b]	3.0[b]	1.20[b]	0.87[b], 0.86[g]	0.74[b], 0.74[g]
ZnTPPS/αCD[b]	0.04	1200	3.3	1.10	0.86	0.75
ZnTPPS/hpαCD[b]	0.04	1200	4.4	0.82	0.86	0.78
ZnTPPS/βCD[b]	0.04	1300	4.4	0.82	0.87	0.75
ZnTPPS/hpβCD[b]	0.04	3200	14.9	0.24	0.82	0.86
ZnTPPS/γCD[b]	0.04	3700	7.9	0.45	0.88	0.74
ZnTPPS/hpγCD[b]	0.05	2500	5.4	0.66	0.89	0.74
TPPC[b]	0.03	80	2.1	1.70	0.78	0.58
TPPC/αCD[b]	0.03	100	2.1	1.70	0.79	0.60
TPPC/hpαCD[b]	0.03	240	4.8	0.74	0.79	0.60
TPPC/βCD[b]	0.03	250	3.9	0.91	0.80	0.60
TPPC/hpβCD[b]	0.03	1300	13.2	0.27	0.85	0.70
TPPC/γCD[b]	0.03	100	3.8	0.95	0.79	0.64
TPPC/hpγCD [b]	0.03	380	4.6	0.77	0.77	0.70
TMPyP	0.046[h]	160[c]	1.8[c]	2.0[c]	0.89[h]	–
TMPyP/hpβCD[c]	0.058	640	1.9	1.9	1.00	–

See Tables 2–5 for definition of symbols and more data on free TPPS and TMPyP.
[a] [162].
[b] [163].
[c] [94].
[d] [120].
[e] [121].
[f] [122].
[g] [177,178].
[h] Average value from [85,168].
[i] [64].

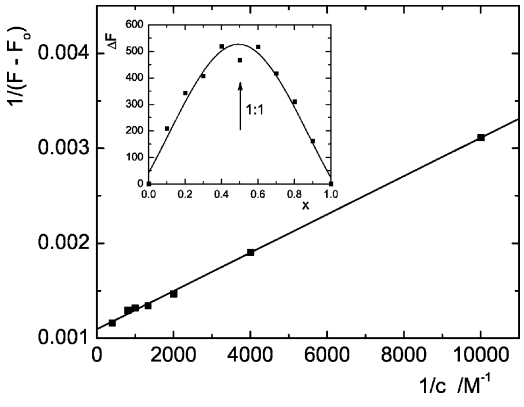

Fig. 9. Benesi–Hildebrand plot for binding of TMPyP by hpβCD. The solid line is the least-squares fit to the experimental data giving the binding constant of $5.4 \times 10^3\ M^{-1}$ in 20 mM phosphate buffer (pH 7.0) at room temperature. Inset: job plot documenting the stoichiometry of the complex to be 1:1.

from the solvation shell of porphyrins and reduction of collisional quenching by solvent molecules from the bulk. Such effects have already been reported for non-covalently attached porphyrins to nucleic acids and proteins (see Section 2.1). Binding also influences the bimolecular rate constant k_q characterizing quenching of the triplet states by oxygen. Quenching by oxygen is a diffusion-controlled process that is slowed down by incorporation of a part of the porphyrin moiety into the cavity. Typical quenching curves recorded in an air-saturated aqueous solution are presented in Fig. 10 showing that the lifetime of the triplet states of the complex increases several times. The complexes of anionic porphyrins with hpβCD, hpγCD, and γCD exhibit the most explicit decrease of k_q. But not even a great excess of αCD or hpαCD (the binding constants of 10^3–$10^4\ M^{-1}$) has any significant influence on the triplet lifetimes in the presence or absence of oxygen. Upon binding of cationic TMPyP with hpβCD the rate constant k_q is not changed since the binding constant is low and the external binding mode shields ^{3}TMPyP from oxygen less than incorporation.

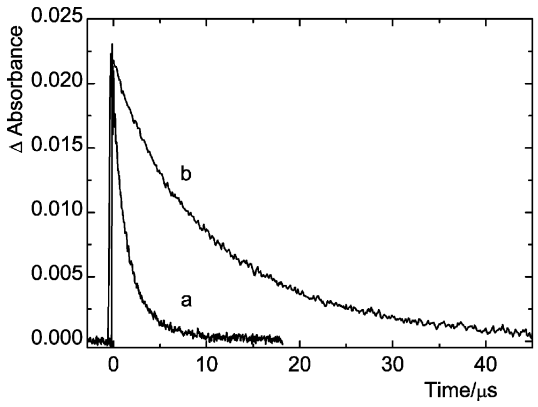

Fig. 10. Traces of the triplet states ^{3}TPPC recorded at 444 nm in the absence (a) and in the presence of 1×10^{-3} M hpβCD (b). Air saturated solutions, 2 μM TPPC, 0.02 M phosphate buffer, pH 7.0.

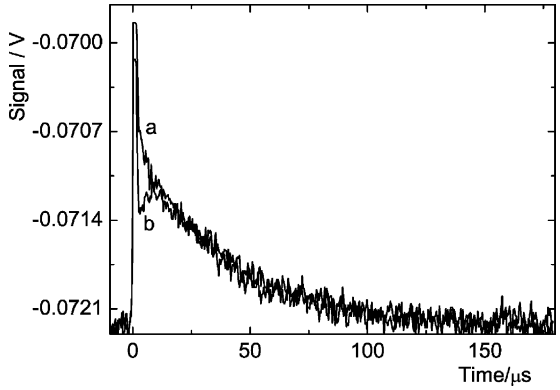

Fig. 11. Formation and decay of $^1O_2$ produced by 2 μM PdTPPS in the absence (a) and in the presence of 1×10^{-3} M hpβCD (b). Optically matched solutions in 90% D_2O at $\lambda_{exc} = 408$ nm, saturated by oxygen, emission traces recorded at 1270 nm, 0.02 M phosphate buffer, pH 7.0.

As a result of the reduced rate constants k_q, the build-up of singlet oxygen concentration produced by the complex is slower than that of free porphyrin (Fig. 11). The quantum yields Φ_Δ, however, are not affected at all (Table 7). Thus, CDs appear to be indifferent molecules. This is in accordance with the fact that CDs have a weak effect on the steady-state concentration of produced $^1O_2$ because the upper limits of bimolecular deactivation constants of $^1O_2$ by βCD and hpβCD are as low as 2×10^5 and 1×10^5 M^{-1} s^{-1}, respectively [169]. The high values of Φ_Δ of the CD complexes indicate that anionic sensitizers TPPS, ZnTPPS, PdTPPS and TPPC retain their sensitizing efficiency [162,163]. For example, the TPPS inclusion complex was found to be an efficient sensitizer with a photooxygenation turnover number up to 30,000 and considerable resistance to photobleaching [170]. By contrast, ZnTPPS is the only reported sensitizer that is quickly photolysed when bound to βCD since the triplet states of bound ZnTPPS participate in competitive electron transfer processes [171,172].

We conclude that the strong non-covalent interaction between CDs and anionic tetraphenylporphyrin sensitizers affects their spectroscopic and photophysical properties such as the bathochromic shift of the Soret band and the lifetimes of the triplet states in the absence or presence of oxygen. However, the inclusion of the porphyrins in the cavity of CDs does not affect the inherent photophysical properties, i.e. the quantum yields Φ_f, Φ_T and Φ_Δ. We presume that, in general, the singlet oxygen producing anionic tetraphenylporphyrins do not lose their sensitizing properties after binding to CDs. Because of the shielding effect of CDs, the bound sensitizers are protected from aggregation and binding to other components in a solution [162,170]. In addition, stable inclusion complexes with linked CD dimers can prevent sensitizer transport by the lipoprotein pathway to healthy tissue and reduce unwanted targeting apart from tumors [173–175]. *The in vitro* phototoxicity of TPPS/hpβCD and ZnTPPS/hpβCD complexes was verified recently [176].

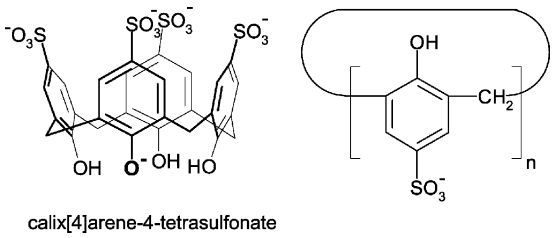

Scheme 8. Molecular structure of sulfonated calixarenes.

2.3.2. *Calix[n]arenes*

Another class of compound capable of encapsulating small molecules are the calix[*n*]arenes. Calix[*n*]arenes are macrocyclic oligophenols linked by methylene bridges (Scheme 8) [179]. Calixarenes adopt a cone conformation both in solid state and in solution. Functionalization of the upper and/or lower rim enables the preparation of conformationally well-defined, rigid or flexible skeletons that may, according to their size and hydrophobicity, selectively include various guest molecules. Weak forces, namely electrostatic interactions, π–π and cation–π interactions play a dominant role. Studies performed in water, where most of the biological processes take place, are of particular relevance.

Water-soluble sulfonatocalixarenes represent flexible and specific hosts for charged or uncharged guests [180,181]. Not much information is available on non-covalently bound porphyrin–calixarene systems in which the importance of the hydrogen bonding [182] and electrostatic interactions [94,183–185] was discovered.

We have described the formation of complexes between cationic TMPyP and sulfonated calixarenes and found that the binding constants and photophysical properties of TMPyP depend on the size of the host [94]. Electrostatic attraction between TMPyP and calixarenes accounts for the high stability of the complexes. Sulfonated calixarenes induce a red shift and a small hypochromicity of the Soret band. The stoichiometry 1:1 for TMPyP-calix[4]arene-4-tetrasulfonate is consistent with charge compensation (ion pairing) of the sulfonate groups and the pyridinium groups

Table 8
The photophysical characteristics of TMPyP bound to water-soluble calix[*n*]arenes [94]

Host	Φ_f	τ_T (μs)	τ (μs)	$k_q \times 10^{-9}$ ($M^{-1}\,s^{-1}$)	Φ_T
Calix[4]arene-4-tetrasulfonate	0.031	75	2.4	1.5	0.57
Calix[6]arene-4-hexasulfonate	0.008	16	2.2	1.6	0.18
Calix[8]arene-4-octasulfonate	0.001	31	2.6	1.4	0.03

See Tables 2, 3 and 7 for explanation of symbols and data on free TMPyP.

on the porphyrin. The hosts—calix[6]arene-4-hexasulfonate and calix[8]arene-4-octasulfonate—are more flexible and, by reason of the structural preorganization into two contrarily oriented cones, two binding sites for TMPyP are disposable. The positive charges of TMPyP compensate the negative charges on the calixarene rims giving the stoichiometry two porphyrins *per* molecule of calixarene.

As discussed in Section 2.1.1.1, the fluorescence emission band of TMPyP is broad (Fig. 8a) with low resolution of the Q(0,0) and Q(0,1) bands caused by an internal photoinduced process. In contrast to the effect described for nucleic acids and CDs, the fluorescence emission spectra of the calixarene complexes are non-structured and are similar to those of the free TMPyP (Fig. 8c–e). Binding to calixarenes quenches fluorescence as indicated by the values of Φ_f in Table 8. The same conclusion follows from time-resolved fluorescence measurements using single photon counting detection. The fluorescence lifetime of 4.9 ns for free TMPyP decreases to 3.6, 1.8 and ~0.7 ns for complexes with calix[4]arene-4-tetrasulfonate, calix[6]arene-4-hexasulfonate and calix[8]arene-4-octasulfonate, respectively. The greatest quenching effect was observed for the complex with calix[8]arene-4-octasulfonate whose Φ_f decreases about 40 times.

The features of the triplet–triplet absorption spectra of TMPyP are not changed upon complexation with calixarenes. The spectra exhibit a broad band with the maximum at 470–490 nm and a negative band caused by bleaching the ground state porphyrin (Fig. 3d). Similar to Φ_f the Φ_T quantum yields of the calixarene complexes are reduced (Table 8). For example the TMPyP complex with calix[8]arene-4-octasulfonate affords a value of Φ_T of 0.03, which is only a fraction of the value measured for free TMPyP ($\Phi_T = 0.89$). Binding is also accompanied by a reduction in the triplet lifetime τ_T (Fig. 12) and by a small decrease of k_q (Table 8) when compared to free TMPyP (Tables 2 and 4).

The Φ_f and Φ_T quantum yields decrease and their sum is considerably lower than 1.0. This fact together with a reduction of the triplet lifetimes was ascribed to intramolecular photoinduced electron transfer between TMPyP and the calixarene [94]. Obviously, the higher is the number of phenol units in the calixarene host the more effective is the quenching of the triplet states signifying that decrease of Φ_T would also diminish Φ_Δ. Of the calixarenes studied, only calix[4]arene-4-tetrasulfonate appears to be a potential host

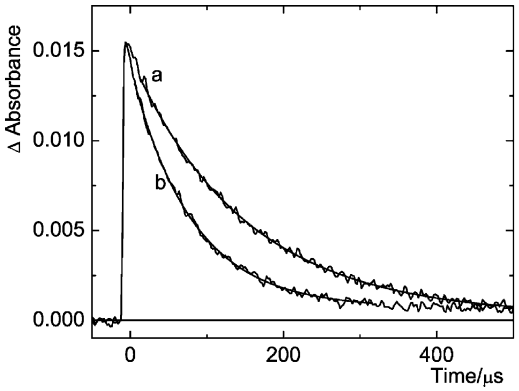

Fig. 12. Decay of the triplet states of TMPyP (a) and of the 1:1 complex with calix[4]arene-4-tetrasulfonate (b). The sample in oxygen-free 20 mM phosphate buffer (pH, 7.0) was excited at 420 nm and the traces were observed at 470 nm. The smooth line is a least-squares fit to the monoexponential function.

for cationic porphyrins because moderate quenching of the triplet states is compensated by the high stability of the complex. These results suggest a promising application of new functionalized calixarenes as sensitizer carriers.

3. Conclusions and outlook

In this review, we have concentrated on porphyrinoid sensitizers the changes of whose photophysical properties have been a consequence of non-covalent interaction with other molecules-biopolymers or abiotic container molecules. From the data summarized throughout the text it can be concluded that the non-covalent interaction of the sensitizers does not restrict the formation of the excited singlet states, triplet states and hence the formation of $^1O_2$ which plays the dominant role in photodynamic processes. Of the photophysical quantities the binding influences spectroscopic properties and kinetic parameters, namely the lifetimes of the excited states and rate constants of collisional quenching. Inherent quantities—Φ_f, Φ_T, Φ_Δ quantum yields—remain mostly unchanged. It is not easy to put forward a general scheme because the overall effect of the photodynamic processes is affected by a combination of numerous, often oppositely acting factors as aggregation, monomerization, compartmentalization, and restriction of internal movements. Moreover, the oxygen independent Type I reactions of the excited states can also contribute to the final photodynamic effect. Taking into consideration all the complexity of the process we have tried to identify the elementary effects of molecules that are constituents of biological systems. A significant condition for the binding is preorganization of the binding sites and/or host molecules, i.e. a conformation change to fit the structure of the interacting guest molecule—the sensitizer. Here, the extent of sensitizer encapsulation, and solvent effects are important namely in assessment of thermodynamics of the

non-covalent interaction (overall free energy of binding, enthalpic and entropic effects) [67,186].

Evidently, the assembling of sensitizers with other molecules is related to molecular recognition. By molecular recognition is generally understood the ability of selective interaction between certain types of molecules in a mixture of various molecules (discrimination between one and another molecule) and formation of a supramolecular assembly [186]. In this context a sensitizer can be viewed as a chromophoric guest. The formation of supramolecular assemblies is relatively simple to achieve and the yields frequently exceed those obtained for the synthesis of analogous covalently bound conjugates since non-covalent interactions involve either entropically or enthalpically driven organization of individual components [187]. The essence of recognition is a non-covalent interaction between molecules since a number of various weak attractive and repulsive forces enables versatility and fine-tuning of properties. The binding can occur provided that the molecules fulfil certain complementarity demands: (i) Geometric complementarity (steric, structural) depending on the size and shape of substituents and cavities (sometimes oversimplified to the lock-and-key concept). (ii) Electronic complementarity comprising all kinds of electronic attraction or repulsion such as Coulombic forces, dipole and multipole interactions, hydrogen bridges or dispersion forces. (iii) Interaction of hydrophobic regions exposed to solvents. (iv) Substitution of labile axial coordination sites of metallocomplexes. Although coordination bonding is not a non-covalent interaction, it plays an important role in recognition and templating as exemplified by the role of zinc porphyrins or DNA metallointercalators [72,188,189]. The non-covalent interactions comprise not only the host and guest molecules but also the molecules of the solvent [73,187]. Among the perspectives that such assemblies offer are custom designed modifications of photosensitizing properties, photochemical stability and binding to specifically directed carriers. There is no principal difference in the influence of abiotic carriers or biopolymers on the interacting sensitizer though biopolymers are much larger molecules with a great variety of binding sites.

In the search for rational understanding of recognition relatively little attention has been dedicated to the kinetics of the partial processes, the basis of kinetic selectivity. The kinetics involve preorganization of hosts (rigidity *versus* flexibility), solvent restructuring (solvation *versus* desolvation, solvent cage changes), and consecutive reactions of supramolecular assemblies (host–guest complex). To disentangle the subtle interplay of kinetic and thermodynamic effects will be a challenging task [186,190].

The obvious application of the reviewed data is in the study of potential carriers and of the mechanism of photodynamic effect in living matter. Similar to slowing down the kinetics of heterogeneous electron transfer reactions after encapsulation [191], the relatively slow kinetics of some photophysical processes can considerably influence the resulting action. Research addressing binding of a sensitizer to a carrier, which is directed to particular receptors in a tumor tissue, i.e. the generation of singlet oxygen in a specified location—are already underway. With the outlook to *in vivo* studies, a number of experiments on the sensitizer triplet states and production of $^1O_2$ was made with cells, tissue samples and microbes [11,192,193]. Even though it is difficult to confirm the assignment of the intermediates produced, because of the relatively low sensitivity of time-resolved methods, these studies offer a good possibility for determining photophysical properties of sensitizers directly in intact tissues. Further development in experimental techniques may bring new views on photodynamic action namely on the specific behaviour of sensitizers *in vivo*. More quantitative data correlating non-covalent interaction and photophysical properties are desirable. Especially data acquired with various porphyrinoid sensitizers are not yet at our disposal. More empirical observations will be clarified on the basis of effects established in simple models and a significant contribution to better comprehension of photodynamic mechanisms in biological systems can be expected from studies of non-covalent binding effects.

Acknowledgements

This research was supported by the Grant Agency of the Czech Republic (grants no. 203/01/0634, 203/02/0420 and 203/02/1483.) We thank the many colleagues, who participated in various parts of the projects described in our review. In particular, we are indebted to Pavel Kubát, Pavel Anzenbacher, Pavel Lhoták, Jan Sejbal and Vladimír Král.

References

[1] R. Nilsson, P.B. Merkel, D.R. Kearns, Photochem. Photobiol. 16 (1972) 117.
[2] C. Schweitzer, R. Schmidt, Chem. Rev. 103 (2003) 1685.
[3] B.M. Aveline, R.W. Redmont, Photochem. Photobiol. 69 (1999) 306.
[4] B.W. Henderson, T.J. Dougherty, Photochem. Photobiol. 55 (1992) 145.
[5] A.E. Lissi, M.V. Encinas, E. Lemp, M.A. Rubio, Chem. Rev. 93 (1993) 699.
[6] F. Riccheli, J. Photochem, Photobiol. B: Biol. 29 (1995) 109.
[7] R.B. Boyle, D. Dolphin, Photochem. Photobiol. 64 (1996) 469.
[8] I.J. MacDonald, T.J. Dougherty, J. Porphyrins Phthalocyanines 5 (2001) 105.
[9] H. Ali, J.E. vanLier, Chem. Rev. 99 (1999) 2379.
[10] C.M. Allen, W.M. Sharman, J.E. vanLier, J. Porphyrins Phthalocyanines 5 (2001) 161.
[11] D. Phillips, in: T.J. Kemp, R.J. Donovan, M.A.J. Rodgers (Eds.), Progress in Reaction Kinetics, vol. 22, 1997, p. 175.
[12] I.B.C. Matheson, J. Lee, J. Am. Chem. Soc. 94 (1972) 3310.
[13] P.R. Ogilby, M. Kristiansen, R.L. Clough, Macromolecules 23 (1990) 2698.
[14] C.S. Foote, Photochem. Photobiol. 54 (1991) 659.
[15] D.M. Wagnerová, Z. Phys. Chem. 215 (2001) 133.
[16] K. Gollnick, Adv. Photochem. 6 (1968) 1.

[17] G. Jori, in: W.M. Horspool, Pill-Soon Song (Eds.), Organic Photochemistry and Photobiology, CRC Press, Boca Raton, Florida, 1995, p. 1379.
[18] A. Harriman, in: W.M. Horspool, Pill-Soon Song (Eds.), Organic Photochemistry and Photobiology, CRC Press, Boca Raton, 1995, p. 1374.
[19] R.V. Bensasson, E.J. Land, T.G. Truscott, Excited States and Free Radicals in Biology and Medicine, Oxford University Press, Oxford, 1993, p. 101.
[20] P.R. Ogilby, Acc. Chem. Res. 32 (1999) 512.
[21] D. Weldon, T.D. Poulsen, K.V. Mikkelsen, P.R. Ogilby, Photochem. Photobiol. 70 (1999) 369.
[22] T. Keszthelyi, D. Weldon, T.A. Andersen, T.D. Poulsen, K.V. Mikkelsen, P.R. Ogilby, Photochem. Photobiol. 70 (1999) 531.
[23] T. Keszthelyi, T.D. Poulsen, P.R. Ogilby, K.V. Mikkelsen, J. Phys. Chem. A 104 (2000) 10550.
[24] C. Schweitzer, Z. Mehrdad, A. Noll, E.W. Grabner, R. Schmidt, J. Phys. Chem. 107 (2003) 2192.
[25] R. Schmidt, M. Bodesheim, Chem. Phys. Lett. 213 (1993) 111.
[26] F. Wilkins, J.G. Brummer, J. Phys. Chem. Ref. Data 10 (1981) 809.
[27] R.Y.N. Ho, J.F. Liebman, J.S. Valentine, in: C.S. Foote, J.S. Valentine, A. Greenberg, J.F. Liebman (Eds.), Active Oxygen in Chemistry, SEARCH Series, vol. 2, Blackie Academic and Professional, London, 1995, p. 1.
[28] L.A. Martinez, C.G. Martínez, B.B. Klopotek, J. Lang, A. Neuner, A.M. Braun, E. Oliveros, J. Photochem. Photobiol. B: Biol. 58 (2000) 94.
[29] C.S. Foote, E.L. Clennan, J.S. Valentine, in: C.S. Foote, J.S. Valentine, A. Greenberg, J.F. Liebman (Eds.), Active Oxygen in Chemistry, SEARCH Series, vol. 2, Blackie Academic and Professional, London, 1995, p. 105.
[30] B.M. Monroe, in: A.A. Frimer (Ed.), Singlet O_2, vol. I, CRC Press, Boca Raton, Florida, 1985, p. 177.
[31] E.L. Clennan, Tetrahedron 56 (2000) 9151.
[32] P. Kubát, K. Lang, J. Mosinger, D.M. Wagnerová, Z. Phys. Chem. 210 (1999) 243.
[33] R. Bonnet, Chem. Soc. Rev. (1995) 19.
[34] J. Cadet, P. Vigny, in: H. Morrison (Ed.), Bioorganic Photochemistry; Photochemistry and the Nucleic Acids, vol. 1, Wiley, New York, 1990, p. 3.
[35] I.E. Kochevar, D.A. Dunn, in: H. Morrison (Ed.), Bioorganic Photochemistry; Photochemistry and the Nucleic Acids, vol. 1, Wiley, New York, 1990, p. 273.
[36] B. Armitage, Chem. Rev. 98 (1998) 1171.
[37] J.L. Ravanat, J. Cadet, Chem. Res. Toxicol. 8 (1995) 379.
[38] S. Stolik, J.A. Delgado, A. Pérez, L. Anasagasti, J. Photochem. Photobiol. B: Biol. 57 (2000) 90.
[39] G. Jori, J. Photochem. Photobiol. A: Chem. 62 (1992) 371.
[40] A.J. MacRoberts, S.G. Bown, D. Phillips, in: Proceedings of the Ciba Foundation Symposium on Photosensitizing Compounds: Their Chemistry, Biology and Clinical Use, vol. 146, Wiley, Chichester, 1989, p. 4.
[41] R.V. Bensasson, E.J. Land, T.G. Truscott, Excited States and Free Radicals in Biology and Medicine, Oxford University Press, Oxford, 1993, p. 342.
[42] G. Jori, in: Proceedings of the Ciba Foundation Symposium on Photosensitizing Compounds: Their Chemistry, Biology and Clinical Use, vol. 146, Wiley, Chichester, 1989, p. 78.
[43] A. Jasat, D. Dolphin, Chem. Rev. 96 (1997) 2267.
[44] I. Rosenthal, Photochem. Photobiol. 53 (1991) 859.
[45] I. Rosenthal, E. Ben-Hur, in: C.C. Leznoff, A.B.P. Lever (Eds.), Phthalocyanines Properties and Applications, VCH Publishers, New York, 1989, p. 393.
[46] M.C. DeRosa, R.J. Crutchley, Coord. Chem. Rev. 233–234 (2002) 351.
[47] D. Wöhrle, J. Gitzel, I. Okura, S. Aono, J. Chem. Soc., Perkin Trans. II (1985) 1171.
[48] E. Vogel, M. Köcher, H. Schmickler, J. Lex, Angew. Chem. Int. Ed. 25 (1986) 257.
[49] E. Vogel, Pure Appl. Chem. 62 (1990) 557.
[50] T.D. Mody, J.L. Sessler, J. Porphyrins Phthalocyanines 5 (2001) 134.
[51] C.G. Claessens, D. González-Rodríguez, T. Torres, Chem. Rev. 102 (2002) 835.
[52] D. Phillips, Pure Appl. Chem. 67 (1995) 117.
[53] K. Lang, P. Kubát, J. Mosinger, D.M. Wagnerová, J. Photochem. Photobiol. A: Chem. 119 (1998) 47.
[54] R.J. Fiel, J.C. Howard, E.H. Mark, N. Datta-Gupta, Nucleic Acids Res. 6 (1979) 3093.
[55] A. Villanueva, J. Photochem. Photobiol. B: Biol. 18 (1993) 295.
[56] P. Kubát, K. Lang, P. Anzenbacher Jr., V. Král, B. Ehrenberg, J. Chem. Soc., Perkin Trans. 1 (2000) 933.
[57] P. Kubát, K. Lang, V. Král, P. Anzenbacher Jr., J. Phys. Chem. B 106 (2002) 6784.
[58] C. Martí, S. Nonell, M. Nicolau, T. Torres, Photochem. Photobiol. 71 (2000) 53.
[59] A. Minnock, D.I. Vernon, J. Schoffield, J. Griffiths, J.H. Parish, S.B. Brown, J. Photochem. Photobiol. B: Biol. 32 (1996) 159.
[60] D.A. Fernández, J. Awruch, L.E. Dicelio, J. Photochem. Photobiol. B: Biol. 41 (1997) 227.
[61] M. Nishio, M. Hirota, Y. Umezawa, The CH/π Interaction; Evidence, Nature, and Consequences, Wiley, New York, 1998, p. 1.
[62] K. Müller-Dethlefs, P. Hobza, Chem. Rev. 100 (2000) 143.
[63] G. Cooke, V.M. Rotello, Chem. Soc. Rev. 31 (2002) 275.
[64] J. Davila, A. Harriman, Photochem. Photobiol. 51 (1990) 9.
[65] K. Lang, D.M. Wagnerová, P. Engst, P. Kubát, Z. Phys. Chem. 187 (1994) 213.
[66] C.G. Claessens, J.F. Stoddart, J. Phys. Org. Chem. 10 (1997) 254.
[67] L. F. Lindoy, I. M. Atkinson, Self-Assembly in Supramolecular Systems. Monographs in Supramolecular Chemistry No. 7, Royal Society of Chemistry, Cambridge, 2000, p. 7.
[68] J.C. Ma, D.A. Dougherty, Chem. Rev. 97 (1997) 1303.
[69] H.-J. Schneider, L. Tianjun, M. Sirish, V. Malinovski, Tetrahedron 56 (2002) 779.
[70] E.V. Rybak-Akimova, Rev. Inorg. Chem. 21 (2001) 207.
[71] J.K.M. Sanders, Pure Appl. Chem. 72 (2000) 2265.
[72] J. Weiss, J. Incl. Phenomena Macrocyclic Chem. 40 (2001) 1.
[73] K. Bhattacharyya, Acc. Chem. Res. 36 (2003) 95.
[74] A.K. Debnath, S. Jiang, N. Strick, K. Lin, P. Haberfield, A.R. Neurath, J. Med. Chem. 37 (1994) 1099.
[75] B. Mestre, M. Pitie, C. Loup, C. Claparols, G. Pratviel, B. Meunier, Nucleic Acids Res. 25 (1997) 1022.
[76] H. Arthanari, S. Basu, T.L. Kawano, P.H. Bolton, Nucleic Acids Res. 26 (1998) 3724.
[77] L. Benimetskaya, G.B. Takle, M. Vilenchik, I. Lebedeva, P. Miller, C.A. Stein, Nucleic Acids Res. 26 (1998) 5310.
[78] R.J. Fiel, J. Biomol. Structure Dynamics 6 (1989) 1259.
[79] R.F. Pasternack, E.J. Gibs, J.J. Villafranca, Biochemistry 22 (1983) 2406.
[80] D.R. McMillin, K.M. McNett, Chem. Rev. 98 (1998) 1201.
[81] P. Lugo-Ponce, D.R. McMillin, Coord. Chem. Rev. 208 (2000) 169.
[82] K. Lang, P. Anzenbacher Jr., P. Kapusta, V. Král, P. Kubát, D.M. Wagnerová, J. Photochem. Photobiol. B: Biol. 57 (2000) 51.
[83] K.E. Thomas, D.R. McMillin, J. Phys. Chem. B 105 (2001) 12628.
[84] S.G. Kruglik, P. Mojzes, Y. Mizutani, T. Kitagawa, P.-Y. Turpin, J. Phys. Chem. B 105 (2001) 5018.
[85] V.S. Chirvony, V.A. Galievsky, N.N. Kruk, B.M. Dzhagarov, P.-Y. Turpin, J. Photochem. Photobiol. B: Biol. 40 (1997) 154.
[86] N.N. Kruk, S.I. Shishporenok, A.A. Korotky, V.A. Galievsky, V.S. Chirvony, P.-Y. Turpin, J. Photochem. Photobiol. B: Biol. 45 (1998) 67.
[87] N.N. Kruk, B.M. Dzhagarov, V.A. Galievsky, V.S. Chirvony, P.-Y. Turpin, J. Photochem. Photobiol. B: Biol. 42 (1998) 181.
[88] A.M. Brun, A. Harriman, J. Am. Chem. Soc. 116 (1994) 10383.

[89] K. Lang, P. Kubát, unpublished results.
[90] N.C. Maiti, S. Mazumbar, N. Periasamy, J. Phys. Chem. B 102 (1998) 1528.
[91] J.M. Kelly, M.J. Murphy, D.J. McConnell, C. OhUigin, Nucleic Acids Res. 13 (1985) 167.
[92] Y. Liu, J.A. Koningstein, Y. Yevdokimov, Can. J. Chem. 69 (1991) 1791.
[93] F.J. Vergeldt, R.B.M. Koehorst, A. vanHoek, T.J. Schaafsma, J. Phys. Chem. 99 (1995) 4397.
[94] K. Lang, P. Kubát, P. Lhoták, J. Mosinger, D.M. Wagnerová, Photochem. Photobiol. 74 (2001) 558.
[95] R. Jasuja, D.M. Jameson, C.K. Nishijo, R.W. Larsen, J. Phys. Chem. B 101 (1997) 1444.
[96] B.P. Hudson, J. Sou, D.J. Berger, D.R. McMillin, J. Am. Chem. Soc. 114 (1992) 8997.
[97] K. Kalyanasundaram, M. Neumann-Spallart, J. Phys. Chem. 86 (1982) 5163.
[98] R.W. Redmond, J.N. Gamlin, Photochem. Photobiol. 70 (1999) 391.
[99] D. Kessel, Cancer Lett. 33 (1986) 183.
[100] U. Muller-Eberhard, W.T. Morgan, Ann. N.Y. Acad. Sci. 244 (1975) 624.
[101] T.G. Gantchev, R. Ouellet, J.E. vanLier, Arch. Biochem. Biophys. 366 (1999) 21.
[102] S. Chatterjee, T.S. Srivastava, J. Porphyrins Phthalocyanines 4 (2000) 147.
[103] J. Davila, A. Harriman, J. Am. Chem. Soc. 112 (1990) 2686.
[104] E. Reddi, F. Ricchelli, G. Jori, Int. J. Peptide Protein Res. 18 (1981) 402.
[105] S.M. Andrade, S.M.B. Costa, Biophys. J. 82 (2002) 1607.
[106] M. Beltramini, P.A. Firey, F. Ricchelli, M.A.J. Rodgers, G. Jori, Biochemistry 26 (1987) 6852.
[107] I.E. Borissevitch, T.T. Tominaga, H. Imasato, M. Tabak, J. Lumin. 69 (1996) 65.
[108] I.E. Borissevitch, T.T. Tominaga, C.C. Schmitt, J. Photochem. Photobiol. A: Chem. 114 (1998) 201.
[109] M.C.S. Foley, A. Beeby, A.W. Parker, S.M. Bishop, D. Phillips, J. Photochem. Photobiol. B: Biol. 38 (1997) 10.
[110] M. Ambroz, A.J. MacRobert, J. Morgan, G. Rumbles, M.S.C. Foley, D. Phillips, J. Photochem. Photobiol. B: Biol. 22 (1994) 105.
[111] J.P. Reyftmann, P. Morliere, S. Goldstein, R. Santus, L. Dubertret, D. Lagrange, Photochem. Photobiol. 40 (1984) 721.
[112] P. Kubát, K. Lang, P. Anzenbacher, Biochim. Biophys. Acta 1670 (2004) 40.
[113] L. Howe, J.Z. Zhang, Photochem. Photobiol. 67 (1998) 90.
[114] E. Mikros, F. Gaudemer, A. Gaudemer, Inorg. Chem. 30 (1991) 1806.
[115] C. Verchere-Beaur, E. Mikros, M. Perree-Fauvet, A. Gaudemer, J. Inorg. Biochem. 40 (1990) 127.
[116] M. Aoudia, M.A.J. Rodgers, J. Am. Chem. Soc. 119 (1997) 12859.
[117] M. Aoudia, A.B. Guliaev, N.B. Leontis, M.A.J. Rodgers, Biophys. Chem. 83 (2000) 121.
[118] A.J. Wilson, K. Groves, R.K. Jain, H.S. Park, A.D. Hamilton, J. Am. Chem. Soc. 125 (2003) 4420.
[119] B.J. White, H.J. Harmon, Biosens. Bioelectron. 17 (2002) 463.
[120] T. Gensch, S.E. Braslavsky, J. Phys. Chem. B 101 (1997) 101.
[121] R. Bonnet, R.J. Ridge, E.J. Land, R.S. Sinclair, D. Tait, T.G. Truscott, J. Chem. Soc., Faraday Trans. I 78 (1982) 127.
[122] F. Wilkinson, W.P. Helman, A.B. Ross, J. Phys. Chem. Ref. Data 22 (1993) 113.
[123] M. Hoebeke, J. Photochem. Photobiol. B: Biol. 28 (1995) 189.
[124] E. Reddi, J. Photochem. Photobiol. B: Biol. 37 (1997) 189.
[125] A.S. Ulrich, Biosci. Reports 22 (2002) 129.
[126] N.G. Angeli, M.G. Lagorio, E.A. San Román, L.E. Dicelio, Photochem. Photobiol. 72 (2000) 49.
[127] A. Blum, L.I. Grossweiner, Photochem. Photobiol. 41 (1985) 27.
[128] V. Gottfried, D. Peled, J.W. Winkelman, S. Kimel, Photochem. Photobiol. 48 (1988) 157.
[129] V.V. Borovkov, M. Anikin, K. Wasa, Y. Sakata, Photochem. Photobiol. 63 (1996) 477.
[130] D. Brault, J. Photochem. Photobiol. B: Biol. 6 (1990) 79.
[131] F. Ricchelli, G. Jori, Photochem. Photobiol. 44 (1986) 151.
[132] P. Sekher, G.M. Garbo, J. Photochem. Photobiol. B: Biol. 20 (1993) 117.
[133] M. Lovčinský, J. Borecký, P. Kubát, P. Ježek, Gen. Physiol. Biophys. 18 (1999) 107.
[134] D. Brault, C. Vever-Bizet, T. Le Doan, Biochim. Biophys. Acta 857 (1986) 238.
[135] L.I. Grossweiner, A.S. Patel, J.B. Grosweiner, Photochem. Photobiol. 36 (1982) 159.
[136] F. Ricchelli, G. Jori, S. Gobbo, M. Tronchin, Biochim. Biophys. Acta 1065 (1991) 42.
[137] B. Ehrenberg, Z. Malik, Y. Nitzan, Photochem. Photobiol. 41 (1985) 429.
[138] M.V. Anikin, V.V. Borovkov, A. Ishida, K. Wasa, Y. Sakata, Chem. Phys. Lett. 226 (1994) 337.
[139] K. Kuzelová, D. Brault, Biochemistry 33 (1994) 9447.
[140] S. Dhami, G. Rumbles, A.J. MacRobert, D. Phillips, Photochem. Photobiol. 65 (1997) 85.
[141] H. Stiel, K. Teuchner, A. Paul, W. Freyer, D. Leupold, J. Photochem. Photobiol. A: Chem. 80 (1994) 289.
[142] M. Craw, R. Redmond, T.G. Truscott, J. Chem. Soc., Faraday Trans. 1 (80) (1984) 2293.
[143] P. Baranyai, S. Gangl, G. Grabner, M. Knapp, G. Köhler, T. Vidóczy, Langmuir 15 (1999) 7577.
[144] X. Damoiseau, F. Tfibel, M. Hoebeke, M.-P. Fontaine-Aupart, Photochem. Photobiol. 76 (2002) 480.
[145] R.C. Straight, J.D. Spikes, Photosensitized oxidation of biomolecules, in: A.A. Frimer (Ed.), Singlet O_2, vol. IV, CRC Press, Boca Raton, Florida, 1985, p. 91.
[146] S. Nonell, S.E. Braslavsky, K. Schaffner, Photochem. Photobiol. 51 (1990) 551.
[147] G. Valduga, S. Nonell, E. Reddi, G. Jori, S.E. Braslavsky, Photochem. Photobiol. 48 (1988) 1.
[148] A. Wiehe, H. Stollberg, S. Runge, A. Paul, M.O. Senge, B. Roder, J. Porphyrins Phthalocyanines 5 (2001) 853.
[149] R.W. Redmond, G. Valduga, S. Nonell, S.E. Braslavsky, K. Schaffner, E. Voegel, K. Pramod, M. Köcher, J. Photochem. Photobiol. B: Biol. 3 (1989) 193.
[150] G. Rossbroich, N.A. Garcia, S.E. Braslavsky, J. Photochem. 31 (1985) 37.
[151] E. Gross, B. Ehrenberg, F.M. Johnson, Photochem. Photobiol. 57 (1993) 808.
[152] A. Lavi, F.M. Johnson, B. Ehrenberg, Chem. Phys. Lett. 231 (1994) 144.
[153] J.D. Spikes, Photochem. Photobiol. 55 (1992) 797.
[154] D.J. Cram, Nature 356 (1992) 29.
[155] A. Jasat, J.C. Sherman, Chem. Rev. 99 (1999) 931.
[156] I. Higler, P. Timmerman, W. Verboom, D. N. Reinhoudt, Eur. J. Org. Chem. (1998) 2689.
[157] J. Szejtli, Chem. Rev. 98 (1998) 1743.
[158] M.V. Rekharsky, Y. Inoue, Chem. Rev. 98 (1998) 1875.
[159] K.A. Connors, Chem. Rev. 97 (1997) 1325.
[160] K. Uekama, F. Hirayama, T. Irie, Chem. Rev. 98 (1998) 2045.
[161] K. Kano, R. Nishiyabu, T. Asada, Y. Kuroda, J. Am. Chem. Soc. 124 (2002) 9937.
[162] J. Mosinger, M. Deumié, K. Lang, P. Kubát, D.M. Wagnerová, J. Photochem. Photobiol. A: Chem. 130 (2000) 13.
[163] J. Mosinger, V. Kliment, J. Sejbal, P. Kubát, K. Lang, J. Porphyrins Phthalocyanines 6 (2002) 514.
[164] Z. El-Hachemi, J.-A. Farrera, H. García-Ortega, O. Ramírez-Gutíerrez, J.M. Ribó, J. Porphyrins Phthalocyanines 5 (2001) 465.
[165] K. Kano, N. Tanaka, H. Minamizono, Y. Kawakita, Chem. Lett. (1996) 925.
[166] J. Mosinger, J. Sejbal, P. Kubát, K. Lang, unpublished results.

[167] F. Venema, A.E. Rowan, R.J.M. Nolte, J. Am. Chem. Soc. 118 (1996) 257.
[168] K. Kalyanasundaram, Inorg. Chem. 23 (1984) 2453.
[169] C.N. Sanramé, R.H. deRossi, G.A. Arguello, Photochem. Photobiol. 68 (1998) 474.
[170] M. Bonchio, T. Carofiglio, M. Carraro, R. Fornasier, U. Tonellato, Org. Lett. 4 (2002) 4635.
[171] S. Mosseri, J.C. Mialocq, Radiat. Phys. Chem. 37 (1991) 653.
[172] S. Mosseri, J.C. Mialocq, B. Perly, J. Phys. Chem. 95 (1991) 2196.
[173] A. Ruebner, J.G. Moser, D. Kirsch, B. Spengler, S. Andrees, S. Roehrs, J. Inclusion Phenom. Mol. Recognition Chem. 25 (1996) 35.
[174] A. Ruebner, D. Kirsch, S. Andrees, W. Decker, B. Roeder, B. Spengler, R. Kaufmann, J.G. Moser, J. Inclusion Phenom. Mol. Recognition Chem. 27 (1997) 69.
[175] J.G. Moser, J. Porphyrins Phthalocyanines 4 (2000) 129.
[176] H. Kolářová, J. Mosinger, R. Lenobel, K. Kejlová, D. Jírová, M. Strnad, Toxicol. In Vitro 17 (2003) 775.
[177] P. Kubát, J. Mosinger, J. Photochem. Photobiol. A 96 (1996) 93.
[178] J. Mosinger, Z. Mička, J. Photochem. Photobiol. A 107 (1997) 77.
[179] C.D. Gutsche, Calixarenes Revisited. The Royal Society of Chemistry, Cambridge, 1998.
[180] S. Shinkai, K. Araki, T. Matsuda, N. Nishiyama, H. Ikeda, I. Takasu, M. Iwamoto, J. Am. Chem. Soc. 112 (1990) 9053.
[181] G. Arena, A. Contino, F.G. Gulino, A. Magri, F. Sansone, D. Sciotto, R. Ungaro, Tetrahedron Lett. 40 (1999) 1597.
[182] A.N. Shivanyuk, D.M. Rudkevich, D.N. Reinhoudt, Tetrahedron Lett. 37 (1996) 9341.
[183] R. Fiammengo, P. Timmerman, F. de Jong, D.N. Reinhoudt, Chem. Commun. (2000) 2313.
[184] L.D. Costanzo, S. Geremia, L. Randaccio, R. Purrello, R. Lauceri, D. Sciotto, F.G. Gulino, V. Pavone, Angew. Chem. Int. Ed. 40 (2001) 4245.
[185] R. Fiammengo, K. Wojciechowski, M. Crego-Calama, P. Timmerman, A. Figoli, M. Wessling, D.N. Reinhoudt, Org. Lett. 5 (2000) 3367.
[186] J.W. Steed, J.L. Atwood, Supramolecular Chemistry, Wiley, Chichester, 2000, p. 8.
[187] F.P. Schmidtchen, Chem. Eur. J. 8 (2002) 3522.
[188] K.E. Erkkila, D.T. Odom, J.K. Barton, Chem. Rev. 99 (1999) 2777.
[189] T. Mitzutani, K. Wada, S. Kitagava, J. Org. Chem. 65 (2000) 6097.
[190] A.E. Kaifer, Acc. Chem. Res. 32 (1999) 62.
[191] C.M. Cardona, S. Mendoza, A.E. Kaifer, Chem. Soc. Rev. 29 (2000) 37.
[192] T.C. Oldham, D. Phillips, A.J. MacRobert, J. Photochem. Photobiol. B: Biol. 61 (2001) 129.
[193] J.A. Lacey, D. Phillips, Phys. Chem. Chem. Phys. 4 (2002) 232.